

Stabilized isogeometric formulation of the Stokes problem on overlapping patches.

Xiaodong Wei^a, Riccardo Puppi^b, Pablo Antolin^b, Annalisa Buffa^b

^a*Shanghai Jiao Tong University - University of Michigan Joint Institute, Shanghai Jiao Tong University, 200240, Shanghai, China*

^b*Institute of Mathematics, École Polytechnique Fédérale de Lausanne, 1015, Lausanne, Switzerland*

Abstract

We present a novel stabilized isogeometric formulation for the Stokes problem, where the geometry of interest is obtained via overlapping NURBS (non-uniform rational B-spline) patches, i.e., one patch on top of another in an arbitrary but predefined hierarchical order. All the visible regions constitute the computational domain, whereas independent patches are coupled through visible interfaces using Nitsche's formulation. Such a geometric representation inevitably involves trimming, which may yield trimmed elements of extremely small measures (referred to as bad elements) and thus lead to the instability issue. Motivated by the minimal stabilization method that rigorously guarantees stability for trimmed geometries [1], in this work we generalize it to the Stokes problem on overlapping patches. Central to our method is the distinct treatments for the pressure and velocity spaces: Stabilization for velocity is carried out for the flux terms on interfaces, whereas pressure is stabilized in all the bad elements. We provide a priori error estimates with a comprehensive theoretical study. Through a suite of numerical tests, we first show that optimal convergence rates are achieved, which consistently agrees with our theoretical findings. Second, we show that the accuracy of pressure is significantly improved by several orders using the proposed stabilization method, compared to the results without stabilization. Finally, we also demonstrate the flexibility and efficiency of the proposed method in capturing local features in the solution field.

This contribution is dedicated to Thomas J.R. Hughes, as a tribute to his remarkable lifetime achievements.

Keywords: Boolean operations, Stokes problem, minimal stabilization, boundary-unfitted method, Nitsche's method

1. Introduction

Isogeometric analysis (IGA) was introduced to bridge the gap between computer-aided design (CAD) and computer-aided engineering (CAE) [2]. Its central idea lies in employing the same basis functions for both design and analysis. IGA typically uses non-uniform rational B-splines (NURBS), the industrial standard of CAD, as basis functions to approximate partial differential equations (PDEs) that govern the physics of interest. In addition to the advancement in the CAD-CAE integration [3, 4, 5], IGA has also

shown great potential in a wide range of applications [6, 7] due to its superior numerical performance in terms of accuracy [8] and robustness [9].

However, directly using CAD models in analysis remains a challenge in IGA due to the ubiquitous trimming operation. NURBS alone is topologically restrictive and can only model box-like geometries. Trimming, essentially a visualization trick that makes part of a geometric model invisible to users, enables modeling geometries of arbitrary topologies in a practically handy way. A CAD model is generally a collection of trimmed NURBS surface patches. In the case of solid modeling, it only represents the boundary of a solid (B-rep) and thus it has no description of its interior domain. On the other hand, the description of the interior domain is often essential for physics-based simulations. There exist several possible ways to bridge this gap. For instance, volumetric parameterization seeks to find a watertight volumetric spline representation conformal to a given B-rep [10, 11, 12], but it usually involves generation of hexahedral meshes, which has been an challenge for decades. Another possibility is through the so-called volume representation (V-rep) [13, 14], where the building blocks are true volumes and naturally have a description of the interior domain, and in the meantime its boundary is a B-rep. The development of analysis-aware and robust volumetric Boolean operations is the key to the success of this road. The third option, which is related to V-reps, is to embed a B-rep to an auxiliary background mesh. Such a geometric representation falls into the category of immersed/unfitted discretizations (e.g., Finite Cell Method [15], cutFEM [16], immersed-isogeometric analysis [6], shifted boundary method [17], aggregated unfitted FEM [18]), where computational meshes do not align with geometric boundaries/interfaces. While geometric modeling is extremely flexible, various issues have to be addressed on the analysis side, such as stability [16, 1, 19, 20], quadrature [21, 22, 23, 24, 25, 26, 27], imposition of boundary conditions [28, 29], conditioning [20], etc. Various methods and applications using trimmed NURBS [30] have been investigated in shells [31, 32] and solid modeling [33]. Interested readers may refer to [20] for a dedicated review on the stability and conditioning issues as well as their treatments.

In this paper, we adopt a general way for geometric construction through overlapping NURBS patches [34] that involves trimming, on which we study the Stokes problem and propose a novel stabilized isogeometric method. The proposed method is a generalization of the minimal stabilization for elliptic problems [1, 34], but it needs distinct treatments for the velocity space and the pressure space. Minimal stabilization is a theoretical framework to deal with the instability issue caused by the cut elements, which are inevitable in trimmed geometries. It was further extended with a conformal layer around boundaries/interfaces to greatly enhance the flexibility of handling boundary/interface conditions [29]. While recently minimal stabilization has been studied for the Stokes problem in a single trimmed patch [35], this paper is focused on multiple overlapping patches, where handling interfaces with a stable formulation plays the key role.

Boundary-unfitted discretizations for the Stokes problem have also been extensively studied in the context of finite element methods. For instances, the inf-sup stability was rigorously shown in [36] for triangular/tetrahedral meshes, rather than being taken as an assumption. Aggregated FEM was also extended to the Stokes problem [37], where additional stabilization terms are added to the mixed finite element spaces to fix the potential deficiencies of the aggregated inf-sup. Recently, high-order FEM was devised and analyzed in [38] for the Stokes interface problem.

The most relevant FEM to our work is the multi-mesh FEM [39, 40], which employs

an overlapping multi-mesh to discretize the computational domain. Both methods adopt Nitsche's method to impose the transmission condition on interfaces. The difference lies in the stabilization: The multi-mesh FEM needs to stabilize over an overlapping domain that consist of both hidden and visible meshes, whereas our method only deals with visible meshes. More specifically, the multi-mesh FEM first finds a mesh intersection for the overlapping domain, which is relatively easy to compute for low-order FEM meshes but becomes much more involving for high-order IGA meshes; see [41] for recent progress. In addition, an least-squares term that involves second-order derivatives is also added to the Nitsche's formulation for the stabilization purpose. On the other hand, our method only counts visible elements/interfaces as the computational domain. It retains the original form of Nitsche's method and only locally modifies certain necessary terms.

The core of the proposed work is to deal with two types of instabilities that arise from the discretizations of the velocity field and the pressure field. Stabilization for velocity is carried out for the flux terms on the interfaces, whereas pressure is stabilized in all the *bad elements*, i.e., elements with a small effective area ratio (up to a given threshold). We rigorously prove the stability of the stabilized formulation and further derive the optimal *a priori* error estimates. In the end, we study several numerical examples to show the convergence and accuracy of the proposed method. Expected optimal convergence is achieved, which consistently agrees with our theoretical results. The accuracy of pressure is significantly improved by several orders compared to the case without stabilization. Furthermore, we also demonstrate the flexibility and efficiency of the proposed method in capturing local features in the solution field.

The paper is structured as follows. After introducing in Section 2 some notations and the model problem, in Section 3 we provide the basic notions that are specific to IGA, describe the construction of overlapping domains through the union operation, and introduce the approximation spaces. In Section 4 we discretize the Stokes problem in a collection of coupled domains with Nitsche's method, and introduce our stabilization procedure together with its key properties and the stabilized discrete formulation. Then, we develop our stability analysis and prove that optimal *a priori* error estimates hold. We provide several numerical experiments in Section 5 to validate the theory. Section 6 concludes the paper and suggests several future directions.

2. Notation and model problem

Let us briefly introduce the definitions and notations which will be frequently employed in this paper. With a slight abuse of notation, we will use the same symbol $|\cdot|$ to denote both the d -dimensional Lebesgue measure and the $(d-1)$ -dimensional Hausdorff measure. Given $D \subset \mathbb{R}^d$ and Σ a hypersurface of \mathbb{R}^d or a subset of it, $|D|$ and $|\Sigma|$ denote the d -dimensional Lebesgue measure of D and the $(d-1)$ -dimensional Hausdorff measure of Σ , respectively. The symbol $\#$ denotes the cardinality of a set. Given $E \subset \mathbb{R}^d$, the notations E° and $\text{int } E$ denote its interior.

A domain is an open, bounded, subset of \mathbb{R}^d , $d \in \{2, 3\}$. A domain D with boundary ∂D is said to be Lipschitz if for every $x \in \partial D$ there exists a neighborhood U of x such that $U \cap \partial D$ is the graph of a Lipschitz function. In the following D denotes a Lipschitz domain with boundary ∂D , and Σ a Lipschitz continuous surface contained in ∂D . The unit outer normal on ∂D is denoted by \mathbf{n} .

We will denote as $\mathbb{Q}_{r,s,t}$ the vector space of trivariate polynomials of degree at most r , s , and t in the first, second, and third variables, respectively (analogously for the case $d = 2$), \mathbb{P}_u the vector space of trivariate polynomials of degree at most u . We may write \mathbb{Q}_k instead of $\mathbb{Q}_{k,k}$ or $\mathbb{Q}_{k,k,k}$. We will often consider the restriction of a polynomial space to a given domain D and write, for instance, $\mathbb{Q}_k(D)$ instead of $\mathbb{Q}_k|_D$.

We denote by $L^2(D)$ the space of square integrable functions on the domain D , equipped with the usual norm $\|\cdot\|_{L^2(D)}$. We denote by $L_0^2(D)$ the subspace of $L^2(D)$ of functions with zero average, where the average of $v \in L^2(D)$ is $\bar{v} := |D|^{-1} \int_D v$.

For a given $\varphi : D \rightarrow \mathbb{R}$ sufficiently regular, α a multi-index with $|\alpha| := \sum_{i=1}^d \alpha_i$, and $j \in \mathbb{N}$, we define $D^\alpha \varphi := \frac{\partial^{|\alpha|} \varphi}{\partial x_1^{\alpha_1} \dots \partial x_d^{\alpha_d}}$ and $\partial_n^j \varphi := \sum_{|\alpha|=j} D^\alpha \varphi \mathbf{n}^\alpha$, where $\mathbf{n}^\alpha := n_1^{\alpha_1} \dots n_d^{\alpha_d}$. We indicate by $H^k(D)$, for $k \in \mathbb{N}$, the standard Sobolev space of functions in $L^2(D)$ whose k -th order weak derivatives belong to $L^2(D)$, equipped with the norm $\|\varphi\|_{H^k(D)}^2 := \sum_{|\eta| \leq k} \|D^\eta \varphi\|_{L^2(D)}^2$. Sobolev spaces of fractional order $H^r(D)$, $r \in \mathbb{R}$, can be defined by interpolation techniques, see [42].

The space $H_{0,\Sigma}^1(D)$ consists of functions in $H^1(D)$ with vanishing trace on Σ . We write $H_0^1(D)$ instead of $H_{0,\partial D}^1(D)$. Let $H^{\frac{1}{2}}(\partial D)$ be the range of the trace operator of functions in $H^1(D)$ and we define its restriction to Σ as $H^{\frac{1}{2}}(\Sigma)$. Both $H^{\frac{1}{2}}(\partial D)$ and $H^{\frac{1}{2}}(\Sigma)$ can be endowed with an intrinsic norm, see [43]. The dual space of $H^{\frac{1}{2}}(\Sigma)$ is denoted by $H^{-\frac{1}{2}}(\Sigma)$. The duality pairing between $H^{\frac{1}{2}}(\Sigma)$ and $H^{-\frac{1}{2}}(\Sigma)$ will be denoted with a formal integral notation. Bold letters will be used for the spaces of vector valued functions.

C will denote generic positive constants that may change with each occurrence throughout the paper but are always independent of the local mesh size, the position of the visible interfaces with respect to the meshes, and the number of patches, unless otherwise specified.

Let Ω be a domain with Lipschitz boundary Γ , with unit outer normal \mathbf{n} , such that $\Gamma = \bar{\Gamma}_D \cup \bar{\Gamma}_N$, where Γ_D and Γ_N are non-empty, open, and disjoint. The Stokes equations are a linear system that can be derived as a simplification of the Navier-Stokes equations. They describe the flow of a fluid under incompressibility and slow motion regimes. Given the body force $\mathbf{f} \in \mathbf{L}^2(\Omega)$, the Dirichlet datum $\mathbf{u}_D \in \mathbf{H}^{\frac{1}{2}}(\Gamma_D)$ and the Neumann datum $\mathbf{u}_N \in \mathbf{H}^{-\frac{1}{2}}(\Gamma_N)$, we look for the *velocity* $\mathbf{u} : \Omega \rightarrow \mathbb{R}^d$ and *pressure* $p : \Omega \rightarrow \mathbb{R}$ such that

$$\begin{aligned} -\mu \Delta \mathbf{u} + \nabla p &= \mathbf{f}, & \text{in } \Omega, \\ \operatorname{div} \mathbf{u} &= 0, & \text{in } \Omega, \\ \mathbf{u} &= \mathbf{u}_D, & \text{on } \Gamma_D, \\ \boldsymbol{\sigma}(\mathbf{u}, p) \mathbf{n} &= \mathbf{u}_N, & \text{on } \Gamma_N, \end{aligned} \tag{1}$$

where $\mu > 0$ is the *viscosity coefficient*, $\boldsymbol{\sigma}(\mathbf{u}, p) := \mu D\mathbf{u} - p\mathbf{I}$ is the *Cauchy stress tensor*, $(D\mathbf{u})_{ij} := \frac{\partial u_i}{\partial x_j}$, $i, j = 1, \dots, d$. The first equation is known as the *conservation of the momentum* and is nothing else than Newton's Second Law, relating the external forces acting on the fluid to the rate of change of its momentum, the second one is the *conservation of mass*. For the sake of simplicity of the notation, let us set $\mu \equiv 1$.

3. Isogeometric analysis on overlapping multipach domains

Before explaining what we mean by “overlapping multipach domains”, let us briefly introduce the basic notions in IGA.

3.1. Univariate splines

Given two positive integers k and n , we say that $\Xi := \{\xi_1, \dots, \xi_{n+k+1}\}$ is a k -open knot vector if

$$\xi_1 = \dots = \xi_{k+1} < \xi_{k+2} \leq \dots \leq \xi_n < \xi_{n+1} = \dots = \xi_{n+k+1}.$$

For the sake of simplicity, we assume $\xi_1 = 0$ and $\xi_{n+k+1} = 1$. We also introduce $Z := \{\zeta_1, \dots, \zeta_M\}$, the set of *breakpoints*, or knots without repetitions, which forms a partition of the unit interval $(0, 1)$. Note that

$$\Xi = \underbrace{\{\zeta_1, \dots, \zeta_1\}}_{m_1 \text{ times}}, \underbrace{\{\zeta_2, \dots, \zeta_2\}}_{m_2 \text{ times}}, \dots, \underbrace{\{\zeta_M, \dots, \zeta_M\}}_{m_M \text{ times}},$$

where m_j is the multiplicity of the breakpoint ζ_j and $\sum_{i=1}^M m_i = n + k + 1$. Moreover, we assume $m_j \leq k$ for every internal knot, and we denote $I_i := (\zeta_i, \zeta_{i+1})$ and its measure $h_i := \zeta_{i+1} - \zeta_i$, $i = 1, \dots, M - 1$.

We denote as $\widehat{B}_{i,k} : [0, 1] \rightarrow \mathbb{R}$ the i th B -spline, $1 \leq i \leq n$, obtained using the *Cox-de Boor formula*

$$\begin{aligned} \widehat{B}_{i,0}(\zeta) &:= \begin{cases} 1, & \text{if } \zeta \in [\xi_i, \xi_{i+1}), \\ 0, & \text{otherwise,} \end{cases} \\ \widehat{B}_{i,k}(\zeta) &:= \frac{\zeta - \xi_i}{\xi_{i+k} - \xi_i} \widehat{B}_{i,k-1}(\zeta) + \frac{\xi_{i+k+1} - \zeta}{\xi_{i+k+1} - \xi_{i+1}} \widehat{B}_{i+1,k-1}(\zeta), \quad k \geq 1, \end{aligned}$$

with the convention that $\frac{0}{0} = 0$. Moreover, let $S_{\alpha}^k(\Xi) := \text{span}\{\widehat{B}_{i,k} : 1 \leq i \leq n\}$ be the vector space of univariate splines of degree k . $S_{\alpha}^k(\Xi)$ can also be characterized as the space of piecewise polynomials of degree k with $\alpha_j := k - m_j$ continuous derivatives at the breakpoints ζ_j , $1 \leq j \leq M$ (*Curry-Schoenberg Theorem* [44]). The number of continuous derivatives at the breakpoints is collected in the *regularity vector* $\alpha := (\alpha_j)_{j=1}^M$. A knot multiplicity $m_j = k + 1$ corresponds to a regularity $\alpha_j = -1$, i.e., a discontinuity at the breakpoint ζ_j . Since the knot vector is open, it holds $\alpha_1 = \alpha_M = -1$. For the sake of simplicity of the notation we assume that the basis functions have the same regularity at the internal knots, namely $\alpha_j = \alpha$ for $2 \leq j \leq M - 1$. Note that the derivatives of splines are splines too when $k \geq 1$ and $\alpha \geq 0$ and, for $\Xi' := \{\xi_2, \dots, \xi_{n+k}\}$, the operator $\frac{d}{dx} : S_{\alpha}^k(\Xi) \rightarrow S_{\alpha-1}^{k-1}(\Xi')$ is surjective, where $\alpha - 1$ denotes the regularity vector $(\alpha_j - 1)_{j=1}^M$.

Moreover, given an interval $I_j = (\zeta_j, \zeta_{j+1}) = (\xi_i, \xi_{i+1})$, we define its *support extension* \widetilde{I}_j as

$$\widetilde{I}_j := \text{int} \bigcup \{\text{supp}(\widehat{B}_{\ell,k}) : \text{supp}(\widehat{B}_{\ell,k}) \cap I_j \neq \emptyset, 1 \leq \ell \leq n\} = (\xi_{i-k}, \xi_{i+k+1}).$$

3.2. Multivariate splines

Let $d \in \{2, 3\}$ denote the space dimension and $M_\ell, n_\ell, k_\ell \in \mathbb{N}$, $\Xi_\ell = \{\xi_{\ell,1}, \dots, \xi_{\ell,n_\ell+k_\ell+1}\}$, $Z_\ell = \{\zeta_{\ell,1}, \dots, \zeta_{\ell,M_\ell}\}$ be given, for every $1 \leq \ell \leq d$. We set the degree vector $\mathbf{k} := (k_1, \dots, k_d)$, the regularity vectors α_ℓ , $1 \leq \ell \leq d$, and $\Xi := \Xi_1 \times \dots \times \Xi_d$. As in the univariate case, we assume that the same regularity holds at the internal knots for every parametric direction, hence we drop the bold font once for all and write α_ℓ , $1 \leq \ell \leq d$. Note that the breakpoints of Z_ℓ form a Cartesian grid in the parametric domain $\widehat{\Omega}$, namely the *parametric Bézier mesh*

$$\widehat{\mathcal{M}}_h := \{Q_{\mathbf{j}} = I_{1,j_1} \times \dots \times I_{d,j_d} : I_{\ell,j_\ell} = (\zeta_{\ell,j_\ell}, \zeta_{\ell,j_\ell+1}) : 1 \leq j_\ell \leq M_\ell - 1\},$$

where each $Q_{\mathbf{j}}$ is called a *parametric Bézier element*, with $h_{Q_{\mathbf{j}}} := \text{diam}(Q_{\mathbf{j}})$. Let $h := \max\{h_Q : Q \in \widehat{\mathcal{M}}_h\}$.

Assumption 1. The family of meshes $\{\widehat{\mathcal{M}}_h\}_h$ is assumed to be shape-regular, that is, the ratio between the smallest edge of $Q \in \widehat{\mathcal{M}}_h$ and its diameter h_Q is uniformly bounded with respect to Q and h .

Remark 1. Shape-regularity implies that the mesh is *locally quasi-uniform*, i.e., the ratio of the sizes of two neighboring elements is uniformly bounded (see [45]). Also note that it allows us to assign h_Q as the unique size of the element, without the necessity of dealing with the length of its edges separately.

Let $\mathbf{I} := \{\mathbf{i} = (i_1, \dots, i_d) : 1 \leq i_\ell \leq n_\ell\}$ be a set of multi-indices. For each $\mathbf{i} = (i_1, \dots, i_d)$, we define the set of *multivariate B-splines* $\{\widehat{B}_{\mathbf{i},\mathbf{k}}(\boldsymbol{\zeta}) = \widehat{B}_{i_1,k_1}(\zeta_1) \dots \widehat{B}_{i_d,k_d}(\zeta_d) : \mathbf{i} \in \mathbf{I}\}$. The *multivariate spline space* in $\widehat{\Omega} := (0,1)^d$ is defined as $S_{\alpha_1, \dots, \alpha_d}^{\mathbf{k}}(\widehat{\mathcal{M}}_h) := \text{span}\{\widehat{B}_{\mathbf{i},\mathbf{k}} : \mathbf{i} \in \mathbf{I}\}$, which can also be seen as the space of piecewise multivariate polynomials of degree \mathbf{k} and regularity $\alpha_1, \dots, \alpha_d$. Note that $S_{\alpha_1, \dots, \alpha_d}^{\mathbf{k}}(\widehat{\mathcal{M}}_h) = \bigotimes_{\ell=1}^d S_{\alpha_\ell}^{k_\ell}(\Xi_\ell)$.

Moreover, for an arbitrary Bézier element $Q_{\mathbf{j}} \in \widehat{\mathcal{M}}_h$, we define its *support extension* $\widetilde{Q}_{\mathbf{j}} := \widetilde{I}_{1,j_1} \times \dots \times \widetilde{I}_{d,j_d}$, where $\widetilde{I}_{\ell,j_\ell}$ is the univariate support extension of the univariate case defined above.

Remark 2. The previous constructions can be easily generalized to the case of Non-Uniform Rational B-Splines (NURBS) basis functions; see, for instance, [46]. For the sake of simplicity of the exposition, in this manuscript we restrict ourselves to the case of B-splines bases.

3.3. Construction of the union domain

Let $\Omega_i^* \subset \mathbb{R}^d$, $0 \leq i \leq N$, with $N \in \mathbb{N}$, $d \in \{2, 3\}$, be spline patches, i.e., $\Omega_i^* = \mathbf{F}_i(\widehat{\Omega})$, where $\mathbf{F}_i \in \left[S_{\alpha_1, \dots, \alpha_d}^{\mathbf{k}}(\widehat{\mathcal{M}}_h)\right]^d$ is the geometric mapping defined by multivariate B-splines and corresponding control points. Each patch has an underlying *premesh* \mathcal{M}_i^* , naturally induced by the map \mathbf{F}_i , namely

$$\mathcal{M}_i^* := \{K \subset \Omega_i^* : K = \mathbf{F}_i(Q), Q \in \widehat{\mathcal{M}}_h\}.$$

For the sake of simplicity of the notation and the analysis, the following simplifications are made.

Assumption 2. We assume that the degree-vector is isotropic and that all predomains are parametrized by splines of the same degree, i.e., $\mathbf{k} = (k, \dots, k)$. Hence, we may write k instead of \mathbf{k} . Similarly for the regularity vectors, that is, $\alpha = \alpha_1 = \dots = \alpha_d$ for all predomains.

Moreover, to prevent the existence of singularities in the parametrizations, we make the following assumption.

Assumption 3. The parametrizations $\mathbf{F}_i : \widehat{\Omega} \rightarrow \Omega_i$, $0 \leq i \leq N$, are bi-Lipschitz. Moreover, $\mathbf{F}_i|_{\overline{Q}} \in C^\infty(\overline{Q})$ for every $Q \in \mathcal{M}_h$ and $\mathbf{F}_i^{-1}|_{\overline{K}} \in C^\infty(\overline{K})$ for every $K \in \mathcal{M}_i^*$, $0 \leq i \leq N$.

Assumption 3 together with Assumption 1 implies that the premeshes \mathcal{M}_i^* , $0 \leq i \leq N$, are shape-regular too.

Let us assume that our computational domain Ω is a *union domain*, namely $\overline{\Omega} = \bigcup_{i=0}^N \overline{\Omega}_i^*$. We define Ω_i as the *visible part* of the predomain Ω_i^*

$$\Omega_i := \Omega_i^* \setminus \bigcup_{\ell=i+1}^N \overline{\Omega}_\ell^*, \quad i = 0, \dots, N.$$

It holds $\Omega_N = \Omega_N^*$ and $\overline{\Omega} = \bigcup_{i=0}^N \overline{\Omega}_i = \bigcup_{i=0}^N \overline{\Omega}_i^*$, see Figure 1. Note that this choice of definition of the Ω_i 's follows [34, 47] and implies a hierarchy of predomains. In particular, if $i > j$ then Ω_i^* is on top of Ω_j^* , in the sense that $\Omega_i^* \cap \Omega_j^*$ is hidden by $\bigcup_{k \geq i} \Omega_k$. We define

$$\Gamma_i := \partial\Omega_i^* \setminus \bigcup_{\ell=i+1}^N \overline{\Omega}_\ell^*, \quad i = 0, \dots, N,$$

i.e., the interface Γ_i is the *visible part of the external boundary* of Ω_i^* with outer unit normal n_i . Moreover, we define the *local interfaces* Γ_{ij} as

$$\Gamma_{ij} := \Gamma_i \cap \overline{\Omega}_j, \quad 0 \leq j < i \leq N,$$

i.e., Γ_{ij} is the subset of the visible boundary of Ω_i^* that intersects Ω_j , see Figure 1(b). We assume that each interface Γ_{ij} either has non-zero $(d-1)$ -measure or is the empty set. We also assume that Γ_{ij} inherits the orientation of Γ_i , hence it has outer unit normal \mathbf{n}_i , also denoted as \mathbf{n} when it is clear from the context which domain is referred to. Note that Γ_{ij} is not connected in general.

Finally, let us make a mild assumption on the roughness of the interfaces Γ_{ij} .

Assumption 4. All the interfaces Γ_{ij} , $1 \leq j < i \leq N$, are Lipschitz-regular.

Lemma 5. There exists $C > 0$ such that, for every $1 \leq j < i \leq N$ and $K \in \mathcal{M}_j$, it holds $|\Gamma_{ij} \cap \overline{K}| \leq Ch_j^{d-1}|_K$.

Proof. This result holds since Γ_{ij} is assumed to be Lipschitz-regular, hence not too oscillating; see [48]. \square

Note that in what follows, we are going to refer to elements $K \in \mathcal{M}_i$, $i = 0, \dots, N$, such that $|\Omega_i \cap K| < |K|$ as *cut elements*. Moreover, integrals and norms will be defined on sets like Γ_{ij} , $\Gamma_{ij} \cap \overline{K}$ and they are meant to be on their interior in a suitable sense.

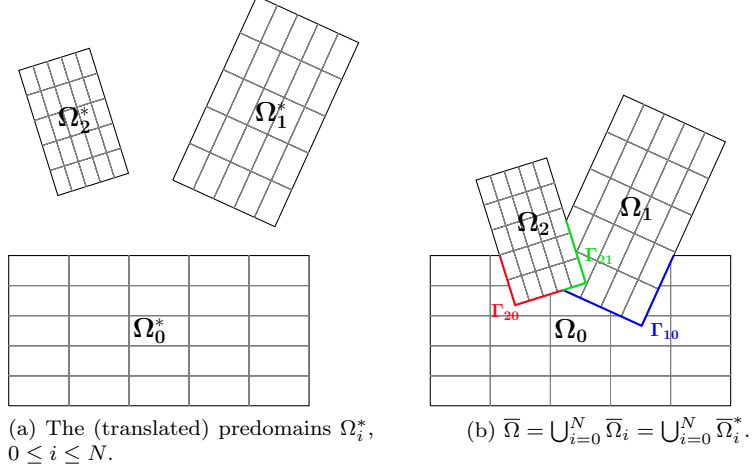


Figure 1: Definitions of predomains (a), visible parts of predomains, and local interfaces (Γ_{10} , Γ_{20} and Γ_{21}) of predomain boundaries (b).

Definition 1. Let $0 \leq j < i \leq N$, and

$$\delta_{ij} := \begin{cases} 1 & \text{if } \Gamma_{ij} \neq \emptyset, \\ 0 & \text{otherwise.} \end{cases}$$

For each $1 \leq i \leq N$, the quantity $\sum_{j=0}^{i-1} \delta_{ij}$ counts the number of visible parts Ω_j whose boundaries are overlapped by Γ_i and, for $0 \leq j \leq N-1$, $\sum_{i=j+1}^N \delta_{ij}$ the number of visible parts whose boundaries overlap Γ_j . We further define $N_\Gamma^\downarrow := \max_{1 \leq i \leq N} \sum_{j=0}^{i-1} \delta_{ij}$, the maximum number of visible parts whose boundaries are overlapped by any visible boundary, and $N_\Gamma^\uparrow := \max_{0 \leq j \leq N-1} \sum_{i=j+1}^N \delta_{ij}$, the maximum number of visible parts whose boundaries cover any visible boundary. Hence, we let $N_\Gamma := \max\{N_\Gamma^\downarrow, N_\Gamma^\uparrow\}$ be the *maximum number of boundary overlaps* in the current configuration.

Definition 2. We let $O_{ij} := \Omega_i \cap \Omega_j^*$, $0 \leq j < i \leq N$, be the *overlap* between the j -th predomain and the i -th visible part. For every $0 \leq j < i \leq N$, we define

$$\eta_{ij} := \begin{cases} 1 & \text{if } O_{ij} \neq \emptyset, \\ 0 & \text{otherwise.} \end{cases}$$

For each $1 \leq i \leq N$, the quantity $\sum_{j=0}^{i-1} \eta_{ij}$ counts the number of predomains covered by the visible part Ω_i . We further define $N_\mathcal{O} := \max_{1 \leq i \leq N} \sum_{j=0}^{i-1} \eta_{ij}$, the maximum number of predomains covered by any visible part.

We observe that $N_\Gamma, N_\mathcal{O} \leq N$; see Figure 2. Moreover, in applications we expect $N_\Gamma, N_\mathcal{O} \ll N$.

We refer to $\mathcal{M}_i := \{K \in \mathcal{M}_i^* : K \cap \Omega_i \neq \emptyset\}$, $i = 0, \dots, N$, as the i -th *active mesh*, consisting of all visible elements (not necessarily fully visible) of the i -th premesh \mathcal{M}_i^* .

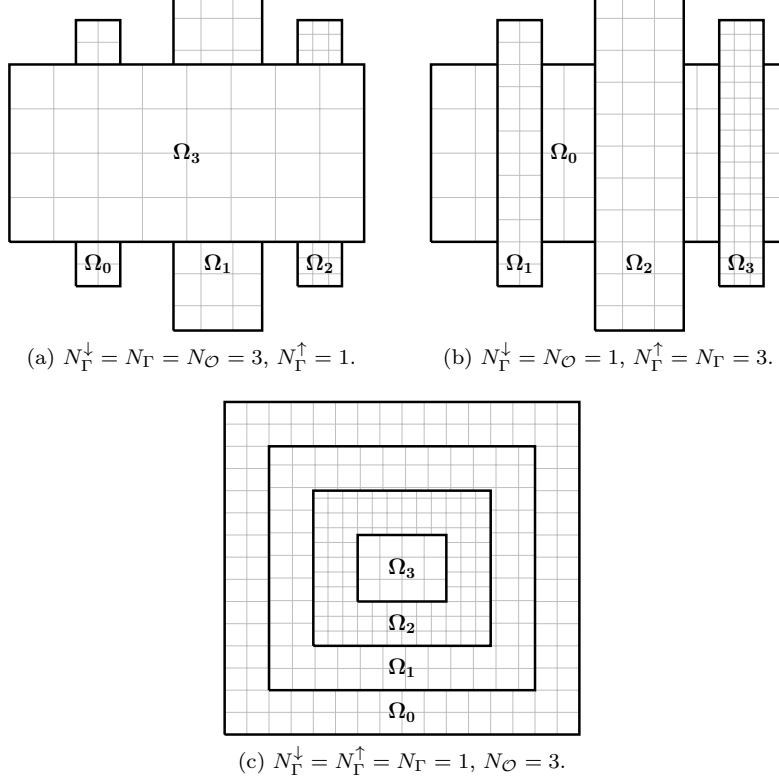


Figure 2: Illustration of N_Γ^\downarrow , N_Γ^\uparrow , N_Γ , $N_\mathcal{O}$.

We define $\mathbf{h}_i : \Omega_i \rightarrow \mathbb{R}^+$ to be the piecewise constant mesh size function of \mathcal{M}_i assigning to each visible element its whole diameter (rather than the diameter of its visible part), namely $\mathbf{h}_i|_{K \cap \Omega} := h_{i,K}$, where $h_{i,K} := \text{diam}(K)$ for every $K \in \mathcal{M}_i$, $0 \leq i \leq N$. Moreover let us denote $h_i := \max_{K \in \mathcal{M}_i} h_{i,K}$ and $h := \max_{0 \leq i \leq N} h_i$ (we use the same notation as for the mesh size of the parametric domain; this is not a dangerous ambiguity since Assumption 3 implies that the local mesh sizes are comparable to the one of the parametric domain). Finally, we denote by $\mathbf{h} : \Omega \rightarrow \mathbb{R}^+$ the piecewise constant function defined as $\mathbf{h}|_{\Omega_i} := \mathbf{h}_i$. Throughout the paper, we are going to rely on the assumption that adjacent sub-domains are discretized with similar mesh sizes.

Assumption 6. *The meshes locally have compatible sizes in the following sense. There exist $c, C > 0$ such that for every $\Gamma_{ij} \neq \emptyset$, with $1 \leq j < i \leq N$, $K_i \in \mathcal{M}_i$ such that $\bar{K}_i \cap \Gamma_{ij} \neq \emptyset$ and $K_j \in \mathcal{M}_j$ such that $\bar{K}_j \cap \Gamma_{ij} \neq \emptyset$, it holds*

$$c\mathbf{h}_j|_{K_j} \leq \mathbf{h}_i|_{K_i} \leq C\mathbf{h}_j|_{K_j}.$$

3.4. Construction of the local approximation spaces

In this section, we construct the isogeometric spaces in the parametric domain.

$$\begin{aligned}\widehat{V}_h^{\text{RT}} &:= \begin{cases} S_{\alpha+1,\alpha}^{k+1,k}(\widehat{\mathcal{M}}_h) \times S_{\alpha,\alpha+1}^{k,k+1}(\widehat{\mathcal{M}}_h), & \text{if } d = 2, \\ S_{\alpha+1,\alpha,\alpha}^{k+1,k,k}(\widehat{\mathcal{M}}_h) \times S_{\alpha,\alpha+1,\alpha}^{k,k+1,k}(\widehat{\mathcal{M}}_h) \times S_{\alpha,\alpha,\alpha+1}^{k,k,k+1}(\widehat{\mathcal{M}}_h), & \text{if } d = 3, \end{cases} \\ \widehat{V}_h^{\text{N}} &:= \begin{cases} S_{\alpha+1,\alpha}^{k+1,k+1}(\widehat{\mathcal{M}}_h) \times S_{\alpha,\alpha+1}^{k+1,k+1}(\widehat{\mathcal{M}}_h), & \text{if } d = 2, \\ S_{\alpha+1,\alpha,\alpha}^{k+1,k+1,k+1}(\widehat{\mathcal{M}}_h) \times S_{\alpha,\alpha+1,\alpha}^{k+1,k+1,k+1}(\widehat{\mathcal{M}}_h) \times S_{\alpha,\alpha,\alpha+1}^{k+1,k+1,k+1}(\widehat{\mathcal{M}}_h), & \text{if } d = 3, \end{cases} \\ \widehat{V}_h^{\text{TH}} &:= \begin{cases} S_{\alpha,\alpha}^{k+1,k+1}(\widehat{\mathcal{M}}_h) \times S_{\alpha,\alpha}^{k+1,k+1}(\widehat{\mathcal{M}}_h), & \text{if } d = 2, \\ S_{\alpha,\alpha,\alpha}^{k+1,k+1,k+1}(\widehat{\mathcal{M}}_h) \times S_{\alpha,\alpha,\alpha}^{k+1,k+1,k+1}(\widehat{\mathcal{M}}_h) \times S_{\alpha,\alpha,\alpha}^{k+1,k+1,k+1}(\widehat{\mathcal{M}}_h), & \text{if } d = 3, \end{cases} \\ \widehat{Q}_h &:= \begin{cases} S_{\alpha,\alpha}^{k,k}(\widehat{\mathcal{M}}_h), & \text{if } d = 2, \\ S_{\alpha,\alpha,\alpha}^{k,k,k}(\widehat{\mathcal{M}}_h), & \text{if } d = 3. \end{cases}\end{aligned}$$

Note that $\widehat{\mathcal{M}}_h$ depends on d . Moreover, spaces of different degrees and regularities on the same parametric mesh $\widehat{\mathcal{M}}_h$ will correspond to different knot vectors. But we do not need to include these details here and we refer the reader to [49] for an in-depth discussion. It holds that $\widehat{V}_h^{\text{RT}} \subset \widehat{V}_h^{\text{N}} \subset \widehat{V}_h^{\text{TH}}$; see [50]. We note that for $\alpha = -1$, $\widehat{V}_h^{\text{RT}}$ and \widehat{V}_h^{N} recover the classical Raviart-Thomas finite element and Nédélec finite element of the second kind, respectively. For $\alpha = 0$, $\widehat{V}_h^{\text{TH}}$ represents the classical Taylor-Hood finite element space. Henceforth we assume $\alpha \geq 0$, and adopt the notation \widehat{V}_h^\square , $\square \in \{\text{RT}, \text{N}, \text{TH}\}$.

For every $0 \leq i \leq N$, we define the local approximation spaces in the patches

$$\begin{aligned}V_{h,i}^{*,\square} &:= \{\mathbf{v}_h : \iota_v^i(\mathbf{v}_h) \in \widehat{V}_h^\square\}, \quad \square \in \{\text{RT}, \text{N}\}, \quad V_{h,i}^{*,\text{TH}} := \{\mathbf{v}_h : \mathbf{v}_h \circ \mathbf{F}_i \in \widehat{V}_h^{\text{TH}}\}, \\ Q_{h,i}^{*,\square} &:= \{q_h : \iota_p^i(q_h) \in \widehat{Q}_h\}, \quad Q_{h,i}^{*,\text{TH}} := \{q_h : q_h \circ \mathbf{F}_i \in \widehat{Q}_h\},\end{aligned}$$

where

$$\begin{aligned}\iota_v^i : \mathbf{H}(\text{div}; \Omega_i^*) &\rightarrow \mathbf{H}(\text{div}; \widehat{\Omega}), & \iota_v^i(\mathbf{v}) &:= \det(D\mathbf{F}_i) D\mathbf{F}_i^{-1}(\mathbf{v} \circ \mathbf{F}_i), \\ \iota_p^i : L^2(\Omega_i^*) &\rightarrow L^2(\widehat{\Omega}), & \iota_p^i(q) &:= \det(D\mathbf{F}_i) (q \circ \mathbf{F}_i).\end{aligned}$$

4. Isogeometric discretization on overlapping multipatch domains

4.1. Nitsche's method for the Stokes problem

We rewrite problem (1) in the following multipatch form. Find $\mathbf{u} : \Omega \rightarrow \mathbb{R}^d$ and $p : \Omega \rightarrow \mathbb{R}$ such that

$$-\text{div } \boldsymbol{\sigma}(\mathbf{u}_i, p_i) = \mathbf{f}, \quad \text{in } \Omega_i, \quad i = 0, \dots, N, \quad (2a)$$

$$-\text{div } \mathbf{u}_i = 0, \quad \text{in } \Omega_i, \quad i = 0, \dots, N, \quad (2b)$$

$$\mathbf{u}_i - \mathbf{u}_j = \mathbf{0}, \quad \text{on } \Gamma_{ij}, \quad 0 \leq j < i \leq N, \quad (2c)$$

$$\boldsymbol{\sigma}(\mathbf{u}_i, p_i) \mathbf{n}_i + \boldsymbol{\sigma}(\mathbf{u}_j, p_j) \mathbf{n}_j = \mathbf{0}, \quad \text{on } \Gamma_{ij}, \quad 0 \leq j < i \leq N, \quad (2d)$$

$$\mathbf{u}_i = \mathbf{u}_D, \quad \text{on } \Gamma_D \cap \Gamma_i, \quad i = 0, \dots, N, \quad (2e)$$

$$\boldsymbol{\sigma}(\mathbf{u}_i, p_i) \mathbf{n}_i = \mathbf{u}_N, \quad \text{on } \Gamma_N \cap \Gamma_i, \quad i = 0, \dots, N, \quad (2f)$$

where $\mathbf{u}_i := \mathbf{u}|_{\Omega_i}$, $p_i := p|_{\Omega_i}$, $i = 0, \dots, N$. Equations (2c) and (2d) are commonly known as *transmission conditions* at the local interfaces.

Proposition 7. *Problems (1) and (2a)–(2f) are equivalent.*

Proof. To demonstrate this result, the variational formulation of the two problems must be used. We refer the interested reader to Chapter 5 of [51]. \square

Let us introduce, for each visible part Ω_i , the *local isogeometric spaces*

$$V_{h,i}^\square := \{\mathbf{v}_h|_{\Omega_i} : \mathbf{v}_h \in V_{h,i}^{*,\square}\}, \quad Q_{h,i}^\square := \{q_h|_{\Omega_i} : q_{h,i} \in Q_{h,i}^{*,\square}\},$$

and glue them to form the *union isogeometric spaces*

$$V_h^\square := \bigoplus_{i=0}^N V_{h,i}^\square, \quad Q_h^\square := \bigoplus_{i=0}^N Q_{h,i}^\square,$$

where $\square \in \{\text{RT}, \text{N}, \text{TH}\}$. To further alleviate the notation, we adopt the convention to denote as V_h the space of the velocities and omit the superscript $\square \in \{\text{RT}, \text{N}, \text{TH}\}$ when what said does not depend from the particular finite element choice. Elements of V_h and Q_h are $(N+1)$ -tuples $\mathbf{v}_h = (\mathbf{v}_0, \dots, \mathbf{v}_N)$ and $q_h = (q_0, \dots, q_N)$, respectively. In practice, we can treat them as ordinary functions thanks to the identification,

$$\begin{aligned} \mathbf{v}_h(x) &= \mathbf{v}_i(x), & \forall x \in \Omega_i, i = 0, \dots, N, \\ q_h(x) &= q_i(x), & \forall x \in \Omega_i, i = 0, \dots, N. \end{aligned}$$

We assume for simplicity that $\partial\Omega$ contains the image of one or more full faces and that Dirichlet boundary conditions are set on full faces only.

Assumption 8. *There exists $0 \leq i \leq N$ such that $\widehat{\Gamma}_i, \widehat{\Gamma}_i := \mathbf{F}_i^{-1}(\Gamma_i)$, contains a full face of the parametric domain $\widehat{\Omega}$. Moreover, for every $0 \leq i \leq N$, $\widehat{\Gamma}_D := \mathbf{F}^{-1}(\Gamma_D)$, $\widehat{\Gamma}_D \cap \widehat{\Gamma}_i$ is either empty or the union of full faces of $\widehat{\Omega}$.*

In case Assumption 8 does not hold, we can combine the technique in this paper with that detailed in [35] to deal with the imposition of Dirichlet boundary conditions in a weak sense.

Let $\varphi : \Omega \rightarrow \mathbb{R}$ be smooth enough and, for every $0 \leq i \leq N$, we denote its restriction to Ω_i as $\varphi_i := \varphi|_{\Omega_i}$. Then, for every interface Γ_{ij} , $0 \leq j < i \leq N$, and a.e. $x \in \Gamma_{ij}$, we define, respectively, the *average* and the *jump* of φ as

$$\langle \varphi \rangle_{t, \Gamma_{ij}}(x) := t\varphi_i|_{\Gamma_{ij}}(x) + (1-t)\varphi_j|_{\Gamma_{ij}}(x), \quad t \in \{\frac{1}{2}, 1\}, \quad (3)$$

$$[\varphi]_{\Gamma_{ij}}(x) := \varphi_i|_{\Gamma_{ij}}(x) - \varphi_j|_{\Gamma_{ij}}(x). \quad (4)$$

We may remove the subscript Γ_{ij} when it is clear from the context to which interface we refer. The average is said to be *symmetric* if $t = \frac{1}{2}$ and *one-sided* when $t = 1$. We define the jump and average of a vector valued function $\boldsymbol{\tau} : \Omega \rightarrow \mathbb{R}^d$ componentwise by letting $\langle \boldsymbol{\tau} \rangle_{t,k} := \langle \tau_k \rangle_t$ and $[\boldsymbol{\tau}]_k := [\tau_k]$, for $0 \leq k \leq d$.

Let us endow V_h and Q_h with the mesh dependent norms:

$$\begin{aligned} \|\mathbf{v}_h\|_{1,h}^2 &:= \sum_{i=0}^N \|D\mathbf{v}_i\|_{L^2(\Omega_i)}^2 + \sum_{i=1}^N \sum_{j=0}^{i-1} \left\| h^{-\frac{1}{2}} [\mathbf{v}_h] \right\|_{L^2(\Gamma_{ij})}^2, & \mathbf{v}_h \in V_h, \\ \|q_h\|_{0,h}^2 &:= \sum_{i=0}^N \|q_i\|_{L^2(\Omega_i)}^2 + \sum_{i=1}^N \sum_{j=0}^{i-1} \left\| h^{\frac{1}{2}} [q_h] \right\|_{L^2(\Gamma_{ij})}^2, & q_h \in Q_h. \end{aligned}$$

We further define

$$V_h^{\mathbf{u}_D} = \{\mathbf{v}_h \in V_h : \mathbf{v}_h|_{\Gamma_D} = \mathbf{u}_D\}, \quad V_h^{\mathbf{0}} = \{\mathbf{v}_h \in V_h : \mathbf{v}_h|_{\Gamma_D} = \mathbf{0}\}.$$

By enforcing the transmission conditions in a weak sense using Nitsche's method, we obtain the following discrete problem.

Find $(\mathbf{u}_h, p_h) \in V_h^{\mathbf{u}_D} \times Q_h$ such that

$$\begin{aligned} a_h(\mathbf{u}_h, \mathbf{v}_h) + b(\mathbf{v}_h, p_h) &= F(\mathbf{v}_h), & \forall \mathbf{v}_h \in V_h^{\mathbf{0}}, \\ b(\mathbf{u}_h, q_h) &= 0, & \forall q_h \in Q_h, \end{aligned} \quad (5)$$

where

$$\begin{aligned} a_h(\mathbf{w}_h, \mathbf{v}_h) &:= \sum_{i=0}^N \int_{\Omega_i} D\mathbf{w}_i : D\mathbf{v}_i - \sum_{i=1}^N \sum_{j=0}^{i-1} \int_{\Gamma_{ij}} (\langle D\mathbf{w}_h \mathbf{n} \rangle_t [\mathbf{v}_h] + [\mathbf{w}_h] \langle D\mathbf{v}_h \mathbf{n} \rangle_t) \\ &\quad + \gamma \sum_{i=1}^N \sum_{j=0}^{i-1} \int_{\Gamma_{ij}} h^{-1} [\mathbf{w}_h] [\mathbf{v}_h], \quad \mathbf{w}_h, \mathbf{v}_h \in V_h, \\ b(\mathbf{v}_h, q_h) &:= - \sum_{i=0}^N \int_{\Omega_i} q_i \operatorname{div} \mathbf{v}_i + \sum_{i=1}^N \sum_{j=0}^{i-1} \int_{\Gamma_{ij}} \langle q_h \rangle_t [\mathbf{v}_h \cdot \mathbf{n}], \quad \mathbf{v}_h \in V_h, q_h \in Q_h, \end{aligned}$$

with $t \in \{\frac{1}{2}, 1\}$, and

$$F(\mathbf{v}_h) := \sum_{i=0}^N \int_{\Omega_i} \mathbf{f} \cdot \mathbf{v}_i + \int_{\Gamma_N} \mathbf{u}_N \cdot \mathbf{v}_h, \quad \mathbf{v}_h \in V_h.$$

Proposition 9. *The discrete variational formulation in Equation (5) is consistent, i.e., the solution (\mathbf{u}, p) of problem (1) satisfies problem (5) as well.*

Proof. The proof is quite standard. See, for instance, Chapter 5 of [51]. \square

Unfortunately, the choice of the parameter γ that guarantees well-posedness of (5) cannot be done independently of how meshes are cut. In the next section, we discuss this issue and propose a suitable stabilization approach.

4.2. Stabilization procedure

As it is well documented in the literature (see e.g., [39, 1, 34]), when there are cut elements, the lack of stability for problem (5) depends on two main issues:

- i) The Nitsche's method requires stabilization. We will adopt the minimal stabilization approach proposed in [1] and successfully used in [34].
- ii) The formulation (5) is not inf-sup stable in presence of small and slim elements. This was observed in e.g., [35]; see also [40].

In what follows, our approach to both i) and ii) will be based on the local extrapolation operators introduced in [1]. We start by introducing the concept of bad element.

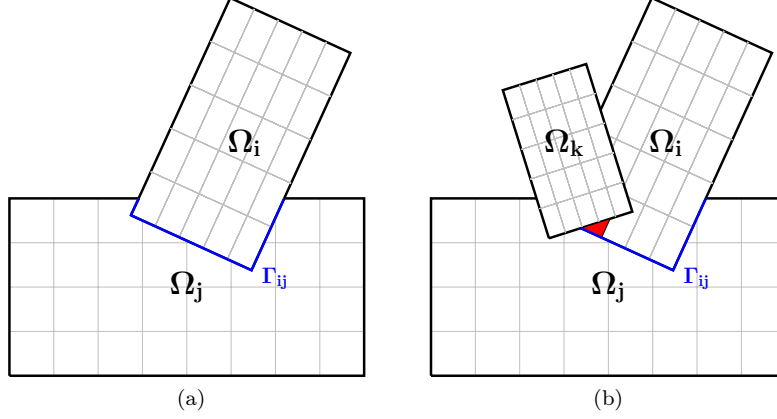


Figure 3: Two-patch and three-patch overlapping along the interface Γ_{ij} .

Definition 3. Fix $\theta \in (0, 1]$, the *area-ratio threshold*. For every $K \in \mathcal{M}_i$, $i = 0, \dots, N$, we say that K is a *good element* if

$$\frac{|\Omega_i \cap K|}{|K|} \geq \theta.$$

Otherwise, K is a *bad element*. We denote as \mathcal{M}_i^g and \mathcal{M}_i^b the collection of good and bad physical Bézier elements, respectively. Note that all the uncut elements in \mathcal{M}_i are good elements, and all its bad elements are cut elements. Moreover, it holds $\mathcal{M}_N^g = \mathcal{M}_N$ (or $\mathcal{M}_N^b = \emptyset$).

Definition 4. Given $K \in \mathcal{M}_i$, $i = 0, \dots, N - 1$, the set of its *neighbors* is

$$\mathcal{N}(K) := \{K' \in \mathcal{M}_k : \text{dist}(K, K') \leq Ch|_K, k = 0, 1, \dots, N\} \setminus \{K\}, \quad (6)$$

where $C > 0$ does not depend on the mesh sizes.

Next, for each bad cut element $K \in \mathcal{M}_i^b$, $0 \leq i < N$, we want to associate a *good neighbor* K' (a neighbor that is a good element). Note that in principle we allow $K' \in \mathcal{M}_k$ with $i \neq k$, i.e., a good neighbor can belong to the mesh of another domain. For every $K \in \mathcal{M}_i^b$, $0 \leq i < N$, its associated good neighbor K' is chosen according to the procedure in Algorithm 1.

Algorithm 1: Find good neighbor

```

Given  $K \in \mathcal{M}_i^b$ ,  $0 \leq i < N$ ;
for  $k = i, \dots, N$  do
    if  $\mathcal{N}(K) \cap \mathcal{M}_k^g \neq \emptyset$  then
         $K' \leftarrow$  any element of  $\mathcal{N}(K) \cap \mathcal{M}_k^g$ ;
        break
    end
end
return  $K'$ ;

```

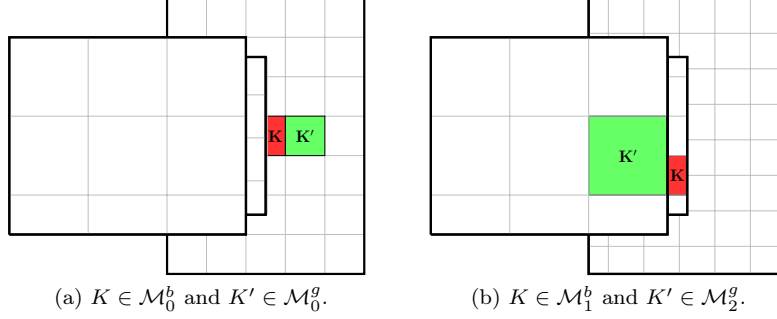


Figure 4: The good neighbor K' located in the same domain as K (a), and in a different (top) domain (b).

If Algorithm 1 does not produce any output, then it suffices to relax the definition of the good neighbor by taking a larger constant C in Definition 4. Figure 4 shows two choices of good neighbor. In Figure 4(b) there is clearly no neighbor of K in \mathcal{M}_1^g , and the algorithm chooses it in \mathcal{M}_2^g .

We remark that, thanks to Assumption 6, the number of times an active element can be chosen as a good neighbor of any other element stays bounded. For this reason, we will not track the dependence of our constant from this number.

The following assumption is not restrictive and is satisfied whenever the meshes of the patches are sufficiently refined, and we take the constant C in (6) large enough.

Assumption 10. *For every $K \in \mathcal{M}_i^b$, $0 \leq i < N$, there exist $i \leq k \leq N$ and $K' \in \mathcal{N}(K) \cap \mathcal{M}_k^g$. From now on we will refer to such K' as a good neighbor of K .*

For every $K \in \mathcal{M}_i^b$, $0 \leq i < N$, its associated good neighbor K' is chosen according to the procedure described in Algorithm 1 in Section 4.2. As already observed, if Algorithm 1 does not produce any output, then it suffices to relax the definition of the good neighbor by taking a larger constant C in (6).

We observe that formulation (5) is well-posed if there are no cut elements, i.e., $\mathcal{M}_k^b = \emptyset$, for every $0 \leq k \leq N$. In the general case $\mathcal{M}_k^b \neq \emptyset$, for some $0 \leq k < N$, the goal of the stabilization is, informally speaking, to extend the stability of the discrete formulation from the internal elements of the visible parts of the patches up to their cut elements.

Let us start by addressing i), i.e., stabilizing the pressure. For $0 \leq j < i \leq N$, $\ell \in \{i, j\}$, let us define $R_\ell^p : Q_h \rightarrow L^2(\Omega_\ell)$ locally. For every $q_h \in Q_h$ and $K \in \mathcal{M}_\ell$, we distinguish two cases:

- if $K \in \mathcal{M}_\ell^g$, then

$$R_\ell^p(q_h)|_K := q_\ell|_K,$$

- if $K \in \mathcal{M}_\ell^b$, then

$$R_\ell^p(q_h)|_K := \mathcal{E}_{K',K}(\Pi_{K'}(q_k|_{K'}))|_K,$$

where $K' \in \mathcal{M}_k^g$ ($\ell \leq k \leq N$), $\Pi_{K'} : L^2(K') \rightarrow \mathbb{Q}_k(K')$ is the L^2 -orthogonal projection onto the space of tensor product polynomials defined on the good neighbor K' , and $\mathcal{E}_{K',K} : \mathbb{Q}_k(K') \rightarrow \mathbb{Q}_k(K \cup K')$ is the canonical polynomial extension. Note

that thanks to the identification $q_h|_{K'} = q_k|_{K'}$. The projection essentially transforms composite spline functions (i.e., splines composite with geometric mapping) to a polynomial representation, which makes the subsequent polynomial extension readily applicable directly in the physical domain. Moreover, functions supported exclusively on badly cut element are removed from the pressure space, and thus projection is necessary.

Lemma 11 (Stability properties of R_ℓ^p). *Given $\theta \in (0, 1]$, there exist $C_{S,1}, C_{S,2} > 0$ such that, for every $0 \leq j < i \leq N$, $K \in \mathcal{M}_\ell$, $\ell \in \{i, j\}$, and $q_h \in Q_h$, we have*

$$\left\| h_\ell^{\frac{1}{2}} R_\ell^p(q_h) \right\|_{L^2(\Gamma_{ij} \cap \bar{K})} \leq C_{S,1} \|q_k\|_{L^2(K' \cap \Omega)}, \quad \|R_\ell^p(q_h)\|_{L^2(K \cap \Omega_\ell)} \leq C_{S,2} \|q_k\|_{L^2(K' \cap \Omega)},$$

where $K' \in \mathcal{M}_k^g$ is a good neighbor of K if $K \in \mathcal{M}_\ell^b$, or $K' = K$ if $K \in \mathcal{M}_\ell^g$.

Proof. The proof is analogous to Theorem 6.4 in [1], so we skip it. \square

The following corollary is an easy consequence of Lemma 11.

Corollary 12. *There exists $C > 0$, depending on N_Γ , such that for every $q_h \in Q_h$, we have*

$$\sum_{i=1}^N \sum_{j=0}^{i-1} \left\| h_\ell^{\frac{1}{2}} [R_{ij}^p(q_h)] \right\|_{L^2(\Gamma_{ij})}^2 \leq C \sum_{i=0}^N \|q_h\|_{L^2(\Omega_i)}^2,$$

where $[R_{ij}^p(q_h)] := R_i^p(q_h)|_{\Gamma_{ij}} - R_j^p(q_h)|_{\Gamma_{ij}}$ for $0 \leq j < i \leq N$.

Now, we propose a minimal stabilization of the bilinear form $a_h(\cdot, \cdot)$. For $0 \leq j < i \leq N$, $\ell \in \{i, j\}$, let us define $R_\ell^v : V_h \rightarrow \mathbf{L}^2(\Omega_\ell)$ locally. For every $\mathbf{v}_h \in V_h$ and $K \in \mathcal{M}_\ell$, we distinguish two cases:

- if $K \in \mathcal{M}_\ell^g$, then

$$R_\ell^v(\mathbf{v}_h)|_K := \mathbf{v}_\ell|_K,$$

- if $K \in \mathcal{M}_\ell^b$, then

$$R_\ell^v(\mathbf{v}_h)|_K := \mathcal{E}_{K',K}(\mathbf{\Pi}_{K'}(\mathbf{v}_k|_{K'}))|_K,$$

where $\mathbf{\Pi}_{K'} : \mathbf{L}^2(K') \rightarrow \mathbb{V}_k(K')$ is the L^2 -orthogonal projection,

$$\mathbb{V}_k(K) := \begin{cases} \mathbb{S}_k(K) & \text{if } \square = \text{RT}, \\ (\mathbb{Q}_{k+1}(K))^d & \text{if } \square \in \{\text{N}, \text{TH}\}, \end{cases}$$

$$\mathbb{S}_k(K) := \begin{cases} \mathbb{Q}_{k+1,k}(K) \times \mathbb{Q}_{k,k+1}(K) & \text{if } d = 2, \\ \mathbb{Q}_{k+1,k,k}(K) \times \mathbb{Q}_{k,k+1,k}(K) \times \mathbb{Q}_{k,k,k+1}(K) & \text{if } d = 3, \end{cases}$$

and $\mathcal{E}_{K',K} : \mathbb{V}_k(K') \rightarrow \mathbb{V}_k(K \cup K')$ is the canonical polynomial extension.

We denote, for $0 \leq j < i \leq N$ such that $\Gamma_{ij} \neq \emptyset$ and $t \in \{\frac{1}{2}, 1\}$,

$$\langle DR_{ij}^v(\mathbf{v}_h)\mathbf{n} \rangle_t := t DR_i^v(\mathbf{v}_h)\mathbf{n}_i|_{\Gamma_{ij}} + (1-t) DR_j^v(\mathbf{v}_h)\mathbf{n}_j|_{\Gamma_{ij}}. \quad (7)$$

In the previous definition, we used the spaces V_h and $V_{h,\ell}$. Let us point out that the stabilization operators R_ℓ^v are equally defined for the spaces with zero boundary conditions V_h^0 and $V_{h,\ell}^0$, $0 \leq \ell \leq N$, as well.

Remark 3. Stabilization of the flux term $\langle DR_{ij}^v(\mathbf{v}_h)\mathbf{n} \rangle_t$ is generally needed for both the symmetric case ($t = \frac{1}{2}$) and the one-sided case ($t = 1$). The symmetric case is straightforward as it involves the flux from a (trimmed) low-level patch. In the one-sided case, however, whether stabilization is needed depends on how many patches are overlapped. If only two patches are overlapped, the flux comes from the (non-trimmed) high-level patch, so there is no need to stabilize. However, if multiple overlapping patches are involved, a certain middle-level patch serves as a high-level patch to the patches below it, so it provides the flux. But at the same time it may be trimmed by the patches on top of it. As a result, the one-sided flux may come from a trimmed patch, so stabilization is needed.

Lemma 13 (Stability property of R_ℓ^v). *Given $\theta \in (0, 1]$, there exists $C > 0$ such that for every $0 \leq j < i \leq N$, $K \in \mathcal{M}_\ell$, $\ell \in \{i, j\}$, and $\mathbf{v}_h \in V_h$, we have*

$$\left\| h_\ell^{\frac{1}{2}} DR_\ell^v(\mathbf{v}_h)\mathbf{n}_\ell \right\|_{L^2(\Gamma_{ij} \cap \bar{K})} \leq C \|D\mathbf{v}_h\|_{L^2(K' \cap \Omega)},$$

where $K' \in \mathcal{M}_k^g$ is a good neighbor of K if $K \in \mathcal{M}_\ell^b$, or $K' = K$ if $K \in \mathcal{M}_\ell^g$.

Proof. We refer the interested reader to its scalar counterpart, i.e., the proof of Theorem 6.4 in [1], or Lemma 3.6 of [34]. \square

Corollary 14. *There exists $C > 0$, depending on N_Γ such that for every $\mathbf{v}_h \in V_h$,*

$$\sum_{i=1}^N \sum_{j=0}^{i-1} \left\| h^{\frac{1}{2}} \langle DR_{ij}^v(\mathbf{v}_h)\mathbf{n} \rangle_t \right\|_{L^2(\Gamma_{ij})} \leq C \sum_{i=0}^N \|D\mathbf{v}_i\|_{L^2(\Omega_i)}$$

Proof. This result is a direct consequence of Lemma 13. \square

We introduce the following stabilized space for the pressures.

$$\begin{aligned} \bar{Q}_h &= \{\varphi_h \in L^2(\Omega) : \exists q_h \in Q_h \text{ such that } \varphi_h|_K = q_h|_K \ \forall K \in \mathcal{M}_i^g \\ &\quad \text{and } \varphi_h|_K = R_h^p(q_h)|_K \ \forall K \in \mathcal{M}_i^b, \forall 0 \leq i \leq N\}. \end{aligned}$$

We can finally propose our stabilized weak formulation.

Find $(\mathbf{u}_h, p_h) \in V_h^{\mathbf{u}^D} \times \bar{Q}_h$ such that

$$\begin{aligned} \bar{a}_h(\mathbf{u}_h, \mathbf{v}_h) + b(\mathbf{v}_h, p_h) &= F(\mathbf{v}_h), \quad \forall \mathbf{v}_h \in V_h^{\mathbf{0}}, \\ b(\mathbf{u}_h, q_h) &= 0, \quad \forall q_h \in \bar{Q}_h, \end{aligned} \tag{8}$$

where

$$\begin{aligned} \bar{a}_h(\mathbf{w}_h, \mathbf{v}_h) &:= \sum_{i=0}^N \int_{\Omega_i} D\mathbf{w}_i : D\mathbf{v}_i - \sum_{i=1}^N \sum_{j=0}^{i-1} \int_{\Gamma_{ij}} (\langle DR_{ij}^v(\mathbf{w}_h)\mathbf{n} \rangle_t [\mathbf{v}_h] + [\mathbf{w}_h] \langle DR_{ij}^v(\mathbf{v}_h)\mathbf{n} \rangle_t) \\ &\quad + \gamma \sum_{i=1}^N \sum_{j=0}^{i-1} \int_{\Gamma_{ij}} h^{-1} [\mathbf{w}_h] [\mathbf{v}_h], \quad \mathbf{w}_h, \mathbf{v}_h \in V_h, \\ b(\mathbf{v}_h, q_h) &:= - \sum_{i=0}^N \int_{\Omega_i} q_i \operatorname{div} \mathbf{v}_i + \sum_{i=1}^N \sum_{j=0}^{i-1} \int_{\Gamma_{ij}} \langle q_h \rangle_t [\mathbf{v}_h \cdot \mathbf{n}], \quad \mathbf{v}_h \in V_h, q_h \in \bar{Q}_h, \end{aligned} \tag{9}$$

with $t \in \{\frac{1}{2}, 1\}$, and

$$F(\mathbf{v}_h) := \sum_{i=0}^N \int_{\Omega_i} \mathbf{f} \cdot \mathbf{v}_i + \int_{\Gamma_N} \mathbf{u}_N \cdot \mathbf{v}_h, \quad \mathbf{v}_h \in V_h.$$

As before $\gamma > 0$ is a penalty parameter scaling as the spline degree of the velocity.

Remark 4. We note that after the discrete pressure space Q_h is altered to the stabilized counterpart \bar{Q}_h , the structure-preserving property of isogeometric Raviart-Thomas elements [52] no longer holds. On the other hand, the difference between Q_h and \bar{Q}_h is localised at cut elements, and so will be the effect of lack of structure preserving properties.

4.3. Interpolation and approximation properties of the discrete spaces

Before analyzing problem (8), we need some technical results. Given a Sobolev function living in the whole physical domain Ω , we consider its restrictions to the predomains Ω_i^* in order to be able to interpolate on each premesh \mathcal{M}_i^* , restrict them in their turn to the visible parts Ω_i , and finally glue together the interpolated functions.

Let us start with the velocity. We construct a quasi-interpolant operator for each local space $V_{h,i}$. Given $\square \in \{\text{RT}, \text{N}, \text{TH}\}$ and $m \geq 1$, for every $i \in \{0, \dots, N\}$, we denote

$$\Pi_{V_h}^{i,\square} : \mathbf{H}^m(\Omega_i) \rightarrow V_{h,i}^\square, \quad \mathbf{v} \mapsto \Pi_{V_h}^{i,\square} \left(\mathbf{v}|_{\Omega_i^*} \right) \Big|_{\Omega_i},$$

where $\Pi_{V_h}^{i,\square} : \mathbf{H}^m(\Omega_i^*) \rightarrow V_{h,i}^{*,\square}$ is a standard quasi-interpolant operator [49, 53]. Then, we glue together the local operators as

$$\Pi_{V_h}^\square : \mathbf{H}^m(\Omega) \rightarrow V_h^\square, \quad \mathbf{v} \mapsto \bigoplus_{i=0}^N \Pi_{V_h}^{i,\square}(\mathbf{v}_i),$$

where $\mathbf{v}_i(x) := \mathbf{v}(x)$ for every $x \in \Omega_i$, $i = 0, \dots, N$. For the pressures, given $r \geq 1$, we introduce the local quasi-interpolants

$$\Pi_{Q_h}^{i,\square} : H^r(\Omega_i) \rightarrow Q_{h,i}^\square, \quad q \mapsto \Pi_{Q_h}^{i,\square} \left(q|_{\Omega_i^*} \right) \Big|_{\Omega_i},$$

where $\Pi_{Q_h}^{i,\square} : H^r(\Omega_i^*) \rightarrow Q_{h,i}^{*,\square}$ is a standard quasi-interpolant operator. We glue together the local operators for the pressures as

$$\Pi_{Q_h}^\square : H^r(\Omega) \rightarrow \bar{Q}_h^\square, \quad q \mapsto R_h^p \left(\bigoplus_{i=0}^N \Pi_{Q_h}^{i,\square}(q_i) \right),$$

where $q_i(x) := q(x)$ for every $x \in \Omega_i$, $i = 0, \dots, N$.

Proposition 15 (Interpolation error estimate). *There exist $C_v, C_p > 0$ such that, for every $(\mathbf{v}, q) \in \mathbf{H}^m(\Omega) \times H^r(\Omega)$, $m \geq 1$ and $r \geq 1$, it holds*

$$\left\| \mathbf{v} - \Pi_{V_h}^\square \mathbf{v} \right\|_{1,h} \leq C_v h^s \|\mathbf{v}\|_{\mathbf{H}^m(\Omega)}, \quad \|q - \Pi_{Q_h}^\square q\|_{0,h} \leq C_p h^\ell \|q\|_{H^r(\Omega)},$$

where $s := \min\{k, m-1\}$ if $\square = \text{RT}$, $s := \min\{k+1, m-1\}$ if $\square \in \{\text{N}, \text{TH}\}$, and $\ell := \min\{k+1, r\}$.

Proof. The proof follows from the best approximation properties of the local quasi-interpolant operators Π_{V_h} ; see e.g., [49]. On the other hand, for Π_{Q_h} , the statement is a direct consequence of Lemma 13, and the fact that, by construction, $R_h^p(\varphi) = \varphi$ for all $\varphi \in \mathbb{Q}_k$. \square

Lemma 16 (Approximation property of R_ℓ^v). *There exists $C > 0$, depending on N_Γ and N_O , such that, for every $\mathbf{v} \in \mathbf{H}^m(\Omega)$, $m \geq 2$, it holds*

$$\sum_{i=1}^N \sum_{j=0}^{i-1} \left\| \mathbf{h}^{\frac{1}{2}} \langle DR_{ij}^v \left(\Pi_{V_h}^\square(\mathbf{v}) \right) \mathbf{n} - D\mathbf{v}\mathbf{n} \rangle_t \right\|_{L^2(\Gamma_{ij})}^2 \leq Ch^{2s} \|\mathbf{v}\|_{\mathbf{H}^m(\Omega)}^2,$$

where $s := \min\{k, m-1\}$ if $\square = \text{RT}$ and $s := \min\{k+1, m-1\}$ if $\square \in \{\text{N}, \text{TH}\}$.

Proof. The proof of such a statement in the scalar case can be found in Proposition 6.9 in [1] and Proposition 4.11 in [35]. \square

4.4. Well-posedness of the stabilized formulation

In order to avoid a direct proof of the inf-sup condition for $b(\cdot, \cdot)$, following [54] and also [35], we reframe the Nitsche formulation as a stabilized Lagrange multiplier method. In doing so, we find a formulation equivalent to (8), but whose well-posedness is easier to prove. First of all, we observe that the transmission conditions at the interfaces (2b) and (2c) can be enforced by introducing a Lagrange multiplier living in $\Lambda := \bigoplus_{0 \leq j < i \leq N} H_{00}^{-\frac{1}{2}}(\Gamma_{ij})$, where, for $0 \leq j < i \leq N$, $H_{00}^{-\frac{1}{2}}(\Gamma_{ij}) := \left(H_{00}^{\frac{1}{2}}(\Gamma_{ij}) \right)'$ and $H_{00}^{\frac{1}{2}}(\Gamma_{ij}) := \{ \varphi \in L^2(\Gamma_{ij}) : \tilde{\varphi} \in H^{\frac{1}{2}}(\Gamma_j) \}$, $\tilde{\varphi}$ denoting the extension by zero of $\varphi \in L^2(\Gamma_{ij})$ on $\Gamma_j \setminus \Gamma_{ij}$ (see Chapter 11 of [55]). Let Λ_h be a discrete subspace of Λ large enough such that, for every $(\mathbf{v}_h, q_h) \in V_h \times \overline{Q}_h$, it holds

$$\mathbf{h}^{-1}[\mathbf{v}_h]|_{\Gamma_{ij}}, \langle DR_{ij}^v(\mathbf{v}_h)\mathbf{n} \rangle_t|_{\Gamma_{ij}}, \langle q_h\mathbf{n} \rangle_t|_{\Gamma_{ij}} \in \Lambda_h, \quad \forall 0 \leq j < i \leq N, t \in \left\{ \frac{1}{2}, 1 \right\}. \quad (10)$$

Our choice is:

$$\Lambda_h := \bigoplus_{0 \leq j < i \leq N} \Lambda_{ij}, \quad \Lambda_{ij} := W_h(\Gamma_{ij}) + L_h(\Gamma_{ij})\mathbf{n} + N_h(\Gamma_{ij})\mathbf{n}, \quad (11)$$

$$\begin{aligned} W_h(\Gamma_{ij}) &:= \{ \mathbf{h}^{-1}\mathbf{w}_h|_{\Gamma_{ij}} : \mathbf{w}_h \in V_h \}, \\ L_h(\Gamma_{ij}) &:= \{ D\mathbf{w}_h|_{\Gamma_{ij}} : \mathbf{w}_h \in V_h \}, \\ N_h(\Gamma_{ij}) &:= \{ \varphi_h|_{\Gamma_{ij}} : \varphi_h \in \overline{Q}_h \}. \end{aligned}$$

It is easy to check that (11) satisfies conditions (10). Moreover, $\Lambda_h \neq \emptyset$. We endow Λ_h with the mesh-dependent norm

$$\|\boldsymbol{\mu}_h\|_{-\frac{1}{2}, h}^2 := \sum_{i=1}^N \sum_{j=0}^{i-1} \left\| \mathbf{h}^{\frac{1}{2}} \boldsymbol{\mu}_h \right\|_{L^2(\Gamma_{ij})}^2, \quad \boldsymbol{\mu}_h \in \Lambda_h.$$

Let us introduce the following stabilized augmented Lagrangian formulation.

Find $(\mathbf{u}_h, p_h, \boldsymbol{\lambda}_h) \in V_h^{\mathbf{u}^D} \times \overline{Q}_h \times \Lambda_h$ such that

$$\overline{\mathcal{A}}_h((\mathbf{u}_h, p_h, \boldsymbol{\lambda}_h); (\mathbf{v}_h, q_h, \boldsymbol{\mu}_h)) = \mathcal{F}(\mathbf{v}_h, q_h, \boldsymbol{\mu}_h), \quad \forall (\mathbf{v}_h, q_h, \boldsymbol{\mu}_h) \in V_h^{\mathbf{0}} \times \overline{Q}_h \times \Lambda_h, \quad (12)$$

where, for $(\mathbf{w}_h, r_h, \boldsymbol{\eta}_h), (\mathbf{v}_h, q_h, \boldsymbol{\mu}_h) \in V_h \times \overline{Q}_h \times \Lambda_h$,

$$\begin{aligned} \overline{\mathcal{A}}_h((\mathbf{w}_h, r_h, \boldsymbol{\eta}_h); (\mathbf{v}_h, q_h, \boldsymbol{\mu}_h)) &:= a(\mathbf{w}_h, \mathbf{v}_h) + b_0(\mathbf{v}_h, r_h) + b_\Gamma(\mathbf{v}_h, \boldsymbol{\eta}_h) \\ &\quad + b_0(\mathbf{w}_h, q_h) + b_\Gamma(\mathbf{w}_h, \boldsymbol{\mu}_h) \\ &\quad - \sum_{i=1}^N \sum_{j=0}^{i-1} \gamma^{-1} \int_{\Gamma_{ij}} \mathbf{h}(\boldsymbol{\eta}_h + \langle DR_{ij}^v(\mathbf{w}_h) \mathbf{n} \rangle_t - \langle r_h \mathbf{n} \rangle_t) (\boldsymbol{\mu}_h + \langle DR_{ij}^v(\mathbf{v}_h) \mathbf{n} \rangle_t - \langle q_h \mathbf{n} \rangle_t), \end{aligned}$$

$$\mathcal{F}(\mathbf{v}_h, q_h, \boldsymbol{\mu}_h) := F(\mathbf{v}_h), \quad a(\mathbf{w}_h, \mathbf{v}_h) := \sum_{i=0}^N \int_{\Omega_i} D\mathbf{w}_i : D\mathbf{v}_i,$$

$$b_0(\mathbf{v}_h, q_h) := - \sum_{i=0}^N \int_{\Omega_i} q_i \operatorname{div} \mathbf{v}_i, \quad b_\Gamma(\mathbf{v}_h, \boldsymbol{\mu}_h) := \sum_{i=1}^N \sum_{j=0}^{i-1} \int_{\Gamma_{ij}} \boldsymbol{\mu}_h [\mathbf{v}_h].$$

Proposition 17. *Let Λ_h be defined as in (11). Then, problem (12) is equivalent to the stabilized Nitsche's formulation (8).*

Proof. We can reformulate problem (12) as follows.

Find $(\mathbf{u}_h, p_h, \boldsymbol{\lambda}_h) \in V_h^{\mathbf{u}^D} \times \overline{Q}_h \times \Lambda_h$ such that

$$\begin{aligned} &a(\mathbf{u}_h, \mathbf{v}_h) + b_0(\mathbf{v}_h, p_h) + b_\Gamma(\mathbf{v}_h, \boldsymbol{\lambda}_h) \\ &- \sum_{i=1}^N \sum_{j=0}^{i-1} \gamma^{-1} \int_{\Gamma_{ij}} \mathbf{h}(\boldsymbol{\lambda}_h + \langle DR_{ij}^v(\mathbf{u}_h) \mathbf{n} \rangle_t - \langle p_h \mathbf{n} \rangle_t) \langle DR_{ij}^v(\mathbf{v}_h) \mathbf{n} \rangle_t = F(\mathbf{v}_h), \quad \forall \mathbf{v}_h \in V_h^{\mathbf{0}}, \\ &b_0(\mathbf{u}_h, q_h) + \sum_{i=1}^N \sum_{j=0}^{i-1} \gamma^{-1} \int_{\Gamma_{ij}} \mathbf{h}(\boldsymbol{\lambda}_h + \langle DR_{ij}^v(\mathbf{u}_h) \mathbf{n} \rangle_t - \langle p_h \mathbf{n} \rangle_t) \langle q_h \mathbf{n} \rangle_t = 0, \quad \forall q_h \in \overline{Q}_h, \\ &b_\Gamma(\mathbf{u}_h, \boldsymbol{\mu}_h) - \sum_{i=1}^N \sum_{j=0}^{i-1} \gamma^{-1} \int_{\Gamma_{ij}} \mathbf{h}(\boldsymbol{\lambda}_h + \langle DR_{ij}^v(\mathbf{u}_h) \mathbf{n} \rangle_t - \langle p_h \mathbf{n} \rangle_t) \boldsymbol{\mu}_h = 0, \quad \forall \boldsymbol{\mu}_h \in \Lambda_h. \end{aligned}$$

From the third equation, we can *statically condensate* the Lagrange multiplier as $\boldsymbol{\lambda}_h =$

$\sum_{i=1}^N \sum_{j=0}^{i-1} \boldsymbol{\lambda}_{ij}$, where

$$\boldsymbol{\lambda}_{ij} = \sum_{i=1}^N \sum_{j=0}^{i-1} \gamma P_{ij} (\mathbf{h}^{-1}[\mathbf{u}_h]) - P_{ij} (\langle DR_{ij}^v(\mathbf{u}_h) \mathbf{n} \rangle_t) + P_{ij} (\langle p_h \mathbf{n} \rangle_t),$$

where $P_{ij} : \mathbf{L}^2(\Gamma_{ij}) \rightarrow \Lambda_{ij}$ is the L^2 -orthogonal projection. By substituting it back to the first and second equations and using (11), we recover the desired formulations. \square

Remark 5. In what follows, we prove the wellposedness of (12) by showing the invertibility of the arising global systems through the so-called *Banach-Nečas-Babuška*

Theorem [56]. On the other hand, we are no longer bound to satisfy an inf-sup condition on the bilinear form $b(\cdot, \cdot)$, and for this reason, we are free to choose the Lagrange multiplier space large enough so that the hypotheses of Proposition 17 are satisfied.

A fundamental ingredient for our numerical analysis is that the following *local inf-sup conditions* are satisfied on each visible part of the domain.

Assumption 18. For every $0 \leq i \leq N$, let us equip $V_{h,i}$ with

$$\|\mathbf{v}_i\|_{1,h,i}^2 := \|D\mathbf{v}_i\|_{L^2(\Omega_i)}^2 + \sum_{k=i+1}^N \left\| \mathbf{h}^{-\frac{1}{2}} \mathbf{v}_i \right\|_{L^2(\Gamma_{ki})}^2 + \sum_{j=0}^{i-1} \left\| \mathbf{h}^{-\frac{1}{2}} \mathbf{v}_i \right\|_{L^2(\Gamma_{ij})}^2, \quad \mathbf{v}_i \in V_{h,i}, \quad (13)$$

and $\overline{Q}_h|_{\Omega_i}$ with $\|\cdot\|_{L^2(\Omega_i)}$. We assume that, for every $0 \leq i \leq N$, there exist β_i such that $\forall q_i \in \overline{Q}_h|_{\Omega_i}$,

$$\sup_{\mathbf{v}_i \in V_{h,i}} \frac{\int_{\Omega_i} q_i \operatorname{div} \mathbf{v}_i}{\|\mathbf{v}_i\|_{1,h,i}} \geq \beta_i \|q_i\|_{L^2(\Omega_i)}. \quad (14)$$

Although we are not able to show a proof of Assumption 18, it is a local result that can be tested. Extensive inf-sup tests are provided in [35], which provide a solid numerical basis for this paper.

The following Lemma provides a norm equivalence result for the space of stabilized pressures, useful for the proof of the inf-sup stability of $b_0(\cdot, \cdot)$.

Lemma 19. There exists $C > 0$ such that

$$\sum_{i=0}^N \|q_i\|_{L^2(\Omega_i)}^2 \leq \|q_h\|_{0,h}^2 \leq C \sum_{i=0}^N \|q_i\|_{L^2(\Omega_i)}^2, \quad \forall q_h \in \overline{Q}_h. \quad (15)$$

Proof. Let us take $q_h \in \overline{Q}_h$. By definition,

$$\|q_h\|_{0,h}^2 = \sum_{i=0}^N \|q_i\|_{L^2(\Omega_i)}^2 + \sum_{i=1}^N \sum_{j=0}^{i-1} \left\| \mathbf{h}^{\frac{1}{2}} [q_h] \right\|_{L^2(\Gamma_{ij})}^2.$$

Hence, we use Proposition 12 so that

$$\|q_h\|_{0,h}^2 \leq C \sum_{i=0}^N \|q_i\|_{L^2(\Omega_i)}^2,$$

where, in particular, C depends on N_Γ and θ . The other inequality trivially holds. \square

The following inf-sup condition for $b_0(\cdot, \cdot)$ is a key ingredient for the proof of the well-posedness of formulation (12).

Lemma 20. Under Assumption 18, given $\theta \in (0, 1]$, there exists $\beta_0 > 0$ such that

$$\inf_{q_h \in \overline{Q}_h} \sup_{\mathbf{v}_h \in V_h} \frac{b_0(\mathbf{v}_h, q_h)}{\|\mathbf{v}_h\|_{1,h} \|q_h\|_{0,h}} \geq \beta_0. \quad (16)$$

Proof. We prove that there exist $C_1, C_2 > 0$ such that, for every $q_h \in \overline{Q}_h$, there exists $\mathbf{v}_h \in V_h$ such that

$$b_0(\mathbf{v}_h, q_h) \geq C_1 \|q_h\|_{0,h}^2, \quad \|\mathbf{v}_h\|_{1,h} \leq C_2 \|q_h\|_{0,h}.$$

Let us fix $q_h := (q_0, \dots, q_N) \in \overline{Q}_h$. From Assumption 18, there exist $C_{1,i}, C_{2,i} > 0$ and $\mathbf{v}_i \in V_{h,i}$, $0 \leq i \leq N$, such that

$$\int_{\Omega_i} q_i \operatorname{div} \mathbf{v}_i \geq C_{1,i} \|q_i\|_{L^2(\Omega_i)}, \quad \|\mathbf{v}_i\|_{1,h,i} \leq C_{2,i} \|q_i\|_{L^2(\Omega_i)}.$$

Let $\mathbf{v}_h := (\mathbf{v}_0, \dots, \mathbf{v}_N)$. By letting $\overline{C}_1 := \min_{0 \leq i \leq N} C_{1,i}$, we have

$$b_0(\mathbf{v}_h, q_h) \geq \overline{C}_1 \sum_{i=0}^N \|q_i\|_{L^2(\Omega_i)}^2.$$

On the other hand, from the Young inequality,

$$\|\mathbf{v}_h\|_{1,h}^2 \leq \sum_{i=0}^N \|D\mathbf{v}_i\|_{L^2(\Omega_i)}^2 + 2 \left(\sum_{i=1}^N \sum_{j=0}^{i-1} \left\| \mathbf{h}^{-\frac{1}{2}} \mathbf{v}_i \right\|_{L^2(\Gamma_{ij})}^2 + \sum_{i=1}^N \sum_{j=0}^{i-1} \left\| \mathbf{h}^{-\frac{1}{2}} \mathbf{v}_j \right\|_{L^2(\Gamma_{ij})}^2 \right).$$

Notice that $\sum_{i=1}^N \sum_{j=0}^{i-1} \left\| \mathbf{h}^{-\frac{1}{2}} \mathbf{v}_j \right\|_{L^2(\Gamma_{ij})}^2 = \sum_{i=0}^{N-1} \sum_{k=i+1}^N \left\| \mathbf{h}^{-\frac{1}{2}} \mathbf{v}_i \right\|_{L^2(\Gamma_{ki})}^2$. Hence, from the definition of $\|\cdot\|_{1,h,i}$ (13) and Assumption 18, it holds

$$\|\mathbf{v}_h\|_{1,h}^2 \leq C \sum_{i=0}^N \|\mathbf{v}_i\|_{1,h,i}^2 \leq \overline{C}_2^2 \sum_{i=0}^N \|q_i\|_{L^2(\Omega_i)}^2, \quad (17)$$

where $\overline{C}_2 := (C\tilde{C})^{\frac{1}{2}}$ and $\tilde{C} := \max_{0 \leq i \leq N} C_{2,i}$. We conclude by taking $C_1 := \overline{C}_1 C^{-1}$ and $C_2 := \overline{C}_2$, where $C > 0$ come from Lemma 19. In particular, note that C depends on θ . \square

Let us indirectly study the well-posedness of the problem (8) by showing that (12) verifies the hypotheses of the so-called Banach-Nečas-Babuška Theorem [56]. The proof of the next result is given in Appendix A.

Theorem 21. *Under Assumption 18, there exists $\overline{\gamma} > 0$ and $C > 0$ such that, for every $\gamma \geq \overline{\gamma}$,*

$$\inf_{(\mathbf{v}_h, q_h, \boldsymbol{\mu}_h) \in V_h \times \overline{Q}_h \times \Lambda_h} \sup_{(\mathbf{w}_h, r_h, \boldsymbol{\eta}_h) \in V_h \times \overline{Q}_h \times \Lambda_h} \frac{\overline{\mathcal{A}}_h((\mathbf{w}_h, r_h, \boldsymbol{\eta}_h); (\mathbf{v}_h, q_h, \boldsymbol{\mu}_h))}{\|(\mathbf{w}_h, r_h, \boldsymbol{\eta}_h)\| \|(\mathbf{v}_h, q_h, \boldsymbol{\mu}_h)\|} \geq C, \quad (18)$$

where $\|\cdot\|$ is the Euclidean product norm on $V_h \times \overline{Q}_h \times \Lambda_h$.

As it is well known (see, e.g., Theorem 3.4.1 in [57]), Theorem 21 implies the well-posedness of problem (12).

We proceed to characterize the existence, uniqueness, and stability for the solution of problem (8) as follows.

Proposition 22. (i) *There exists $\bar{\gamma} > 0$ such that, for every fixed $\gamma \geq \bar{\gamma}$, there exists $M_a > 0$ such that*

$$|\bar{a}_h(\mathbf{w}_h, \mathbf{v}_h)| \leq M_a \|\mathbf{w}_h\|_{1,h} \|\mathbf{v}_h\|_{1,h}, \quad \forall \mathbf{w}_h, \mathbf{v}_h \in V_h.$$

(ii) *There exists $\alpha > 0$ such that, for every $\gamma \geq \bar{\gamma}$,*

$$\alpha \|\mathbf{v}_h\|_{1,h}^2 \leq \bar{a}_h(\mathbf{v}_h, \mathbf{v}_h), \quad \forall \mathbf{v}_h \in \ker B,$$

where $\ker B := \{\mathbf{v}_h \in V_h : b(\mathbf{v}_h, q_h) = 0, \quad \forall q_h \in \bar{Q}_h\}$.

(iii) *There exists $M_b > 0$ such that*

$$|b(\mathbf{v}_h, q_h)| \leq M_b \|\mathbf{v}_h\|_{1,h} \|q_h\|_{0,h}, \quad \forall \mathbf{v}_h \in V_h, \forall q_h \in \bar{Q}_h.$$

(iv) *There exists $\beta > 0$ such that*

$$\inf_{q_h \in \bar{Q}_h} \sup_{\mathbf{v}_h \in V_h} \frac{b(\mathbf{v}_h, q_h)}{\|\mathbf{v}_h\|_{1,h} \|q_h\|_{0,h}} \geq \beta.$$

(v) *There exists $M_F > 0$ such that*

$$|F(\mathbf{v}_h)| \leq M_F \|\mathbf{v}_h\|_{1,h}, \quad \forall \mathbf{v}_h \in V_h.$$

Conditions (i)-(v) hold if and only there exists a unique solution (\mathbf{u}_h, p_h) of (8). Moreover,

$$\|\mathbf{u}_h\|_{1,h} \leq \frac{1}{\alpha} \|F\|_{-1,h}, \quad \|p_h\|_{0,h} \leq \frac{1}{\beta} \left(1 + \frac{M_a}{\alpha}\right) \|F\|_{-1,h}, \quad (19)$$

where $\|\cdot\|_{-1,h}$ denotes the dual norm with respect to $\|\cdot\|_{1,h}$.

Proof. This is a standard result; see, for instance, Theorem 3.4.1 in [57]. \square

Theorem 23. *Under Assumption 18, given $\theta \in (0, 1]$, there exists a unique solution $(\mathbf{u}_h, p_h) \in V_h^{\mathbf{u}^D} \times \bar{Q}_h$ of the stabilized problem (8) satisfying (19).*

Proof. From Theorem 21 there exists a unique solution $(\mathbf{u}_h, p_h, \boldsymbol{\lambda}_h) \in V_h^{\mathbf{u}^D} \times \bar{Q}_h \times \Lambda_h$ of (12). Thanks to Proposition 17, (\mathbf{u}_h, p_h) is the unique solution of problem (8). \square

4.5. A priori error estimates

The goal of this section is to demonstrate that the errors, for both the velocity and pressure fields, achieve optimal *a priori* convergence rates in the topologies induced by the norms $\|\cdot\|_{1,h}$ and $\|\cdot\|_{0,h}$, respectively.

Lemma 24. *Given $\theta \in (0, 1]$, let $(\mathbf{u}, p) \in \mathbf{H}^{\frac{3}{2}+\varepsilon}(\Omega) \times L^2(\Omega)$, $\varepsilon > 0$, and $(\mathbf{u}_h, p_h) \in V_h \times \bar{Q}_h$ be the solutions to (1) and (8), respectively. Then, for every $(\mathbf{u}^I, p^I) \in V_h \times \bar{Q}_h$,*

the following estimates hold.

$$\begin{aligned}
\|\mathbf{u}_h - \mathbf{u}^I\|_{1,h} &\leq \frac{1}{\alpha} \left(M_a \|\mathbf{u} - \mathbf{u}^I\|_{1,h} + \sum_{i=1}^N \sum_{j=0}^{i-1} \left\| \mathbf{h}^{\frac{1}{2}} \langle D(\mathbf{u} - R_{ij}^v(\mathbf{u}^I)) \mathbf{n} \rangle_t \right\|_{L^2(\Gamma_{ij})} \right. \\
&\quad \left. + M_b \|p - p^I\|_{0,h} \right) + \frac{1}{\beta} \left(1 + \frac{M_a}{\alpha} \right) M_b \|\mathbf{u} - \mathbf{u}^I\|_{1,h}, \\
\|p_h - p^I\|_{0,h} &\leq \frac{1}{\beta} \left(1 + \frac{M_a}{\alpha} \right) \left(M_a \|\mathbf{u} - \mathbf{u}^I\|_{1,h} + \sum_{i=1}^N \sum_{j=0}^{i-1} \left\| \mathbf{h}^{\frac{1}{2}} \langle D(\mathbf{u} - R_{ij}^v(\mathbf{u}^I)) \mathbf{n} \rangle_t \right\|_{L^2(\Gamma_{ij})} \right. \\
&\quad \left. + M_b \|p - p^I\|_{0,h} \right) + \frac{M_a}{\beta^2} \left(1 + \frac{M_a}{\alpha} \right) M_b \|\mathbf{u} - \mathbf{u}^I\|_{1,h}.
\end{aligned}$$

Proof. Let us fix $(\mathbf{u}^I, p^I) \in V_h \times \overline{Q}_h$. By linearity $(\mathbf{u}_h - \mathbf{u}^I, p_h - p^I) \in V_h \times \overline{Q}_h$ satisfies the saddle point problem

$$\begin{aligned}
\bar{a}_h(\mathbf{u}_h - \mathbf{u}^I, \mathbf{v}_h) + b(\mathbf{v}_h, p_h - p^I) &= F^I(\mathbf{v}_h), \quad \forall \mathbf{v}_h \in V_h^0, \\
b(\mathbf{u}_h - \mathbf{u}^I, q_h) &= G^I(q_h), \quad \forall q_h \in \overline{Q}_h,
\end{aligned} \tag{20}$$

where, for every $(\mathbf{v}_h, q_h) \in V_h^0 \times \overline{Q}_h$,

$$\begin{aligned}
F^I(\mathbf{v}_h) &:= \sum_{i=0}^N \int_{\Omega_i} D(\mathbf{u} - \mathbf{u}^I) : D\mathbf{v}_h - \sum_{i=1}^N \sum_{j=0}^{i-1} \int_{\Gamma_{ij}} (\langle D(\mathbf{u} - R_{ij}^v(\mathbf{u}^I)) \mathbf{n} \rangle_t [\mathbf{v}_h] \\
&\quad + \langle DR_{ij}^v(\mathbf{v}_h) \mathbf{n} \rangle_t [\mathbf{u} - \mathbf{u}^I]) + \gamma \sum_{i=1}^N \sum_{j=0}^{i-1} \int_{\Gamma_{ij}} \mathbf{h}^{-1} [\mathbf{u} - \mathbf{u}^I] [\mathbf{v}_h] + b(\mathbf{v}_h, p - p^I), \\
G^I(q_h) &:= b(\mathbf{u} - \mathbf{u}^I, q_h).
\end{aligned}$$

It is sufficient to apply the stability estimates (19) to the solution $(\mathbf{u}_h - \mathbf{u}^I, p_h - p^I)$ of (20). \square

Theorem 25. Under Assumption 18, given $\theta \in (0, 1]$, let $(\mathbf{u}, p) \in \mathbf{H}^m(\Omega) \times H^r(\Omega)$, $m \geq 2$ and $r \geq 1$, be the solution to problem (1). Then, the discrete solution $(\mathbf{u}_h, p_h) \in V_h^{\square, \mathbf{u}^D} \times \overline{Q}_h^{\square}$ of the stabilized problem (8) satisfies

$$\|\mathbf{u} - \mathbf{u}_h\|_{1,h} + \|p - p_h\|_{0,h} \leq Ch^{\min\{s, \ell\}} \left(\|\mathbf{u}\|_{H^m(\Omega)} + \|p\|_{H^r(\Omega)} \right),$$

where $s := \min\{k, m - 1\}$ if $\square = \text{RT}$, $s := \min\{k + 1, m - 1\}$ if $\square \in \{\text{N}, \text{RT}\}$, $\ell := \min\{k + 1, r\}$, and $C > 0$ depends on the constants appearing in Lemma 24.

Proof. It is sufficient to proceed by triangular inequality and apply Proposition 15, and Lemma 16. \square

5. Numerical examples

In this section, we present several numerical examples to demonstrate the convergence, accuracy, conditioning, and efficiency of the proposed method. The viscosity coefficient

is $\mu = 1$. Taylor-Hood elements are used for the discretization. The threshold of $\theta = 0.1$ is used to identify bad elements. The creation of an interface quadrature mesh follows exactly the same as [34], where the key is to find a mesh intersection on the boundary of the top patch such that each quadrature cell only involves polynomials. The reparameterization of cut elements for numerical integration follows that of [29], where each cut element is decomposed into a collection of primitive cells (i.e., high-order triangles and/or quadrilaterals).

5.1. Two-patch union

We start with a two-patch union that can control the trimming condition via a single parameter ϵ . As the input, the bottom (B-spline) patch is simply a unit square with a grid of 8×8 elements, whereas the top patch is a trapezoid with 5×5 elements; see Figure 5. Note that the horizontal and vertical boundaries of the top patch align with certain mesh lines of the bottom patch. As ϵ decreases, the effective area of cut elements shrinks, i.e., the trimming condition deteriorates.

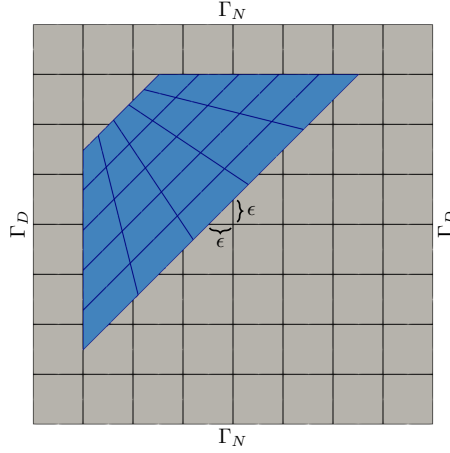


Figure 5: The initial mesh and boundary conditions of the two-patch union.

We adopt the following manufactured solution for the convergence study,

$$\mathbf{u} = \begin{bmatrix} 2e^x(-1+x)^2x^2(y^2-y)(-1+2y) \\ -e^x(-1+x)x(-2+3x+x^2)(-1+y)^2y^2 \end{bmatrix},$$

and

$$p = -424 + 156e + (y^2 - y)(-456 + e^x(456 + x^2(228 - 5(y^2 - y)) \\ + 2x(-228 + y^2 - y) + 2x^3(-36 + y^2 - y) + x^4(12 + y^2 - y))).$$

Boundary conditions are imposed on the bottom patch. The Dirichlet boundary condition ($\mathbf{u} = \mathbf{0}$) is imposed on the left and right boundaries, whereas the Neumann boundary condition is imposed on the top and bottom boundaries.

We first check the convergence in an extremely trimmed case with $\epsilon = 10^{-12}$. Quadratic and cubic spline discretizations (for pressure) are studied. A series of consecutively refined meshes is obtained for the convergence study by globally refining both top and

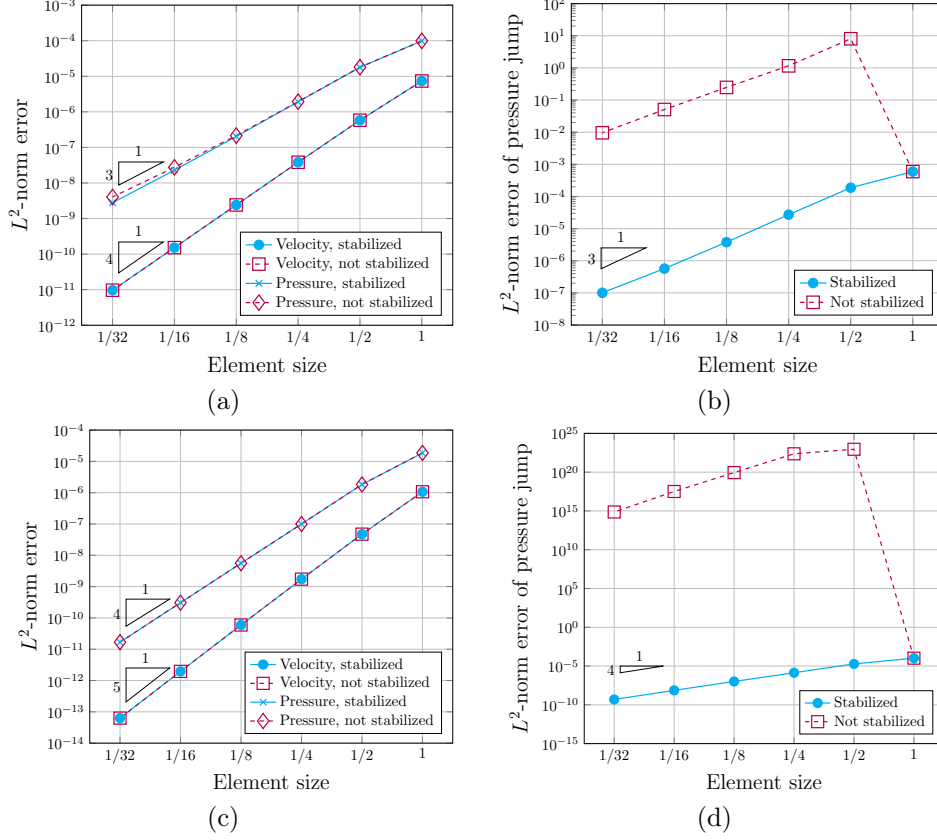


Figure 6: Convergence plots of the two-patch union with $\epsilon = 10^{-12}$. (a, b) Quadratic spline discretization (for pressure), and (c, d) cubic spline discretization (for pressure).

bottom patches. The symmetric flux is adopted on the interface. The results are summarized in Figure 6. We compute two kinds of error: Figure 6(a, c) corresponds to the error in the patch interior without considering the interface, whereas Figure 6(b, d) is the error on the interface. In Figure 6(a, c), we observe that expected optimal convergence rates are achieved in all cases, regardless of whether bad elements are stabilized or not. In fact, the accuracy (in terms of the L^2 -norm error) is almost indistinguishable. However, when looking at the accuracy of the pressure jump across the interface in Figure 6(b, d), we find a significant difference of 5 orders (the quadratic case) or 26 orders (the cubic case). This means that without stabilization, the approximation error of pressure jump blows up at the interface. This behavior was not observed in the elliptic problems [34]. It signifies the necessity of stabilizing bad elements in general problems also for the sake of accuracy.

We next study the influence of stabilization on the conditioning of the resulting linear system. The test is carried out with a fixed mesh resolution but a varying trimming condition by changing ϵ ; see Figure 5. The symmetric flux is adopted. The quadratic discretization (for pressure) is used. Condition numbers are computed from precondi-

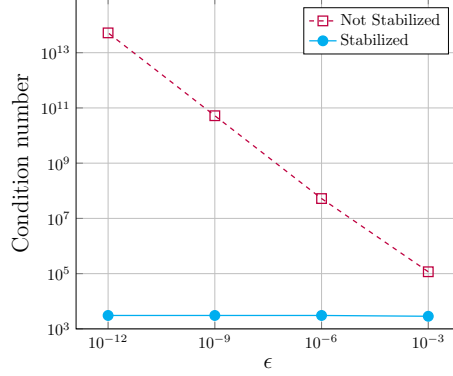


Figure 7: Conditioning with respect to the trimming condition (ϵ).

tioned matrices, where we use the diagonal preconditioner. The results are summarized in Figure 7. We observe that in the non-stabilized case, the condition numbers quickly blow up (in the order of $10^5 \sim 10^{13}$) as ϵ decreases. In contrast, the condition numbers remain a constant ($\sim 10^3$) in the stabilized case regardless of the change of ϵ , which numerically verifies the efficacy of the proposed stabilization method.

It is worth mentioning that regarding the conditioning issue, two types of cut elements are distinguished in a recent review article on stability and conditioning [20]: one that contains a single vertex (Case 1), and the other that contains no vertex at all (Case 2). According to the particular treatment of cut elements in [20], the conditioning issue in Case 1 can be resolved by merely rescaling the stiffness matrix with a Jacobi preconditioner, whereas Case 2 needs both stabilization and rescaling. While our example here “geometrically” belongs to Case 1, it exhibits a fundamental difference due to the different treatment of cut elements. There is only one basis function in [20], which is also the condition for rescaling only to resolve the conditioning issue, whereas there are always multiple basis functions in our example. Indeed, based on the results in Figure 7, where the condition numbers are computed on rescaled matrices, we conclude that, unfortunately, rescaling only does not work in our case and stabilization is essential.

5.2. Multi-patch union

Next we study whether the number of overlapping patches has a negative impact on accuracy. The overall geometry is simply a unit square, over which we gradually increase the number of overlapping patches from 2 to 5; see Figure 8. To create a complex multi-patch overlapping scenario, each time we place a new patch in such a way that it overlaps with all the existing patches, which in practice becomes more and more difficult to achieve as the number of patches increases. All patches are intended to have a similar resolution. This way, the overall mesh, i.e., the collection of the visible meshes of all patches, can relatively retain a similar resolution even if new patches are added.

We compare the accuracy for meshes of different number of overlaps. Using the same manufactured solution in Section 5.1, we check the convergence as well as accuracy. The initial meshes are shown in Figure 8. The convergence plots are summarized in Figure 9. We observe that expected optimal convergence is achieved in all cases. In fact, the

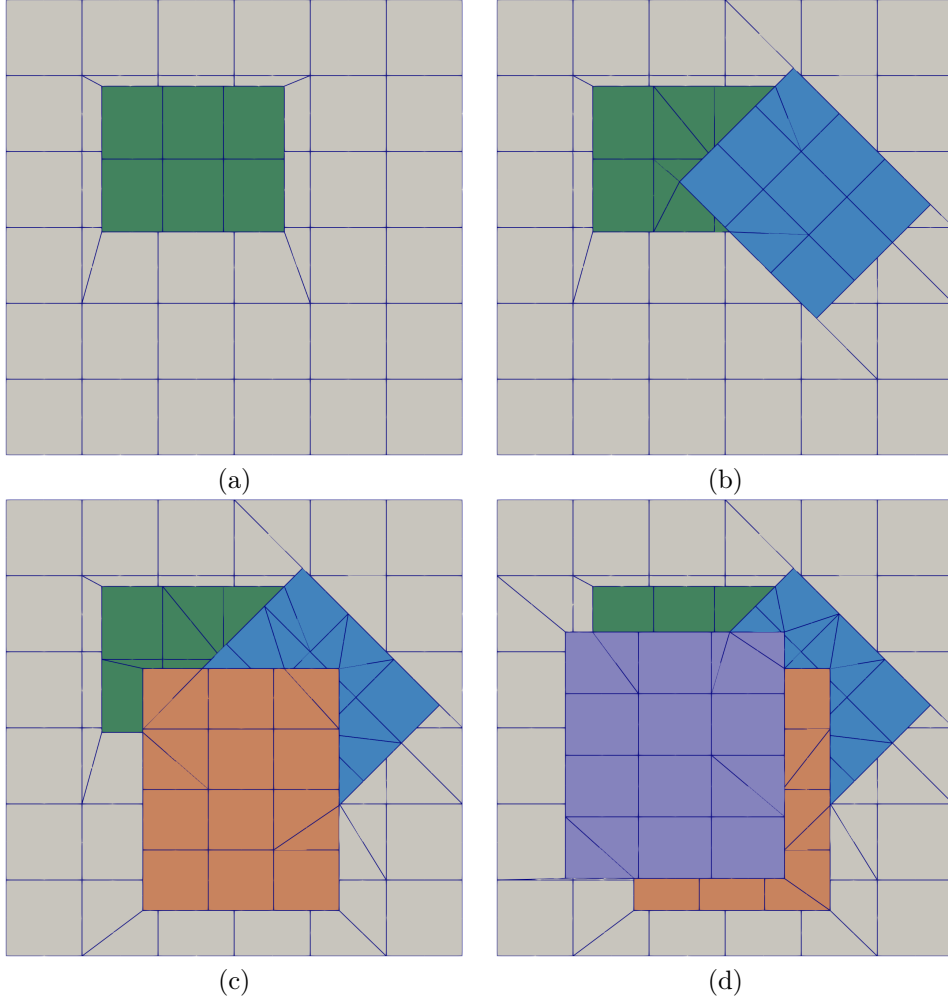


Figure 8: Multiple overlapping patches: Initial meshes. Note that trimmed elements may be reparameterized into multiple integration cells.

accuracy of both velocity and pressure are almost indistinguishable, especially when the meshes are fine enough (e.g., $h \leq 1/4$ with h being the element size). This means that the number of overlapping patches does not have an important effect on accuracy when the number is moderate. In practice, having a large number of overlaps (under the condition that each patch overlaps with all the patches below it) is quite rare to encounter.

5.3. Airfoil

In the last example, we solve the Stokes problem around an airfoil to show the flexibility and efficiency of the proposed method in capturing local features in the solution field. We compare two geometric constructions, one via straightforward trimming, and the other using the immersed boundary-conformal method (IBCM) [29]; see Figure 10.

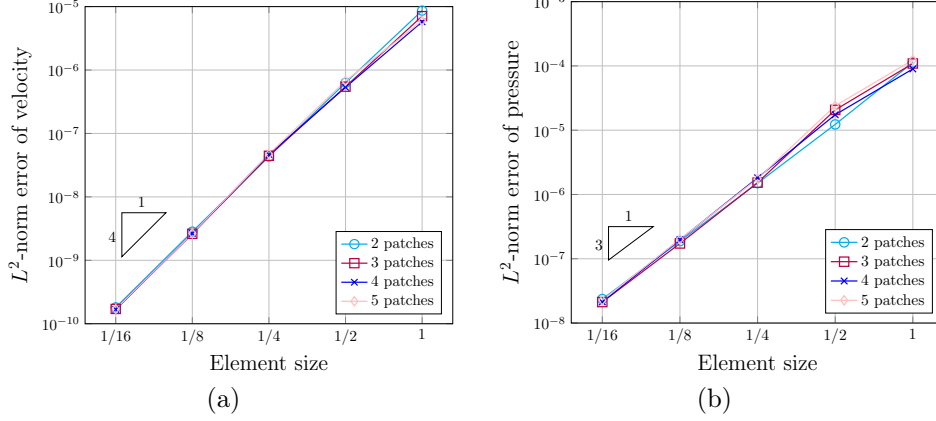


Figure 9: Initial meshes of multiple overlapping patches, where the number of patches varies. Note that trimmed elements may be reparameterized into multiple integration cells.

IBCM is a special type of overlapping construction that features a layer of conformal mesh around geometric features (e.g., boundaries or interfaces), while keeping the majority of the computational domain described by the Cartesian grid. This way, IBCM represents a hybrid manner of geometric modeling that leverages the advantages of both the boundary-fitted method and the boundary-unfitted method.

The geometric modeling using IBCM for this example is introduced as follows. The initial data of the airfoil is a series of points, to which we fit a quadratic B-spline curve Γ_{airfoil} . An offset B-spline curve Γ_{offset} is then obtained by offsetting the control polygon of Γ_{airfoil} . This way we can readily have a layer of conformal mesh. We adopt such a simple way for offsetting because as already shown in [29], the shape of the offset curve does not influence much the accuracy. Finally, Γ_{offset} is used to trim the background Cartesian grid. The computational domain consists of the conformal mesh and the trimmed Cartesian grid.

The boundary conditions are shown in Figure 10(a). A parabolic Dirichlet condition is imposed on the left side, the homogeneous Dirichlet condition is imposed on the top and bottom boundaries as well as the airfoil, and the homogeneous Neumann condition is imposed on the right side. Quadratic spline discretization (for pressure) is used for this problem. We are particularly interested in the pressure field because it has a large gradient at the left tip of the airfoil and exhibits a singularity at the right tip.

We first compare the pressure fields using the initial meshes shown in Figure 10(b, c). The results are shown in Figure 11(a, b). We observe that with trimming, as the mesh does not align with the airfoil geometry and the mesh resolution is not fine enough, the pressure at the two ends of the airfoil is poorly resolved. On the other hand, with IBCM, since its mesh aligns with the airfoil, it can already capture the large gradient even with a low mesh resolution. In fact, to achieve a comparable accuracy as IBCM (using the initial mesh), the trimming construction has to dyadically refine its initial mesh at least three times. The result is shown as a zoom-in view in Figure 11(c). For easy comparison, the same zoom-in view of the IBCM result is shown in Figure 11(d).

Moreover, in Figure 12 we plot the pressure along the line $y = 0$ using meshes of

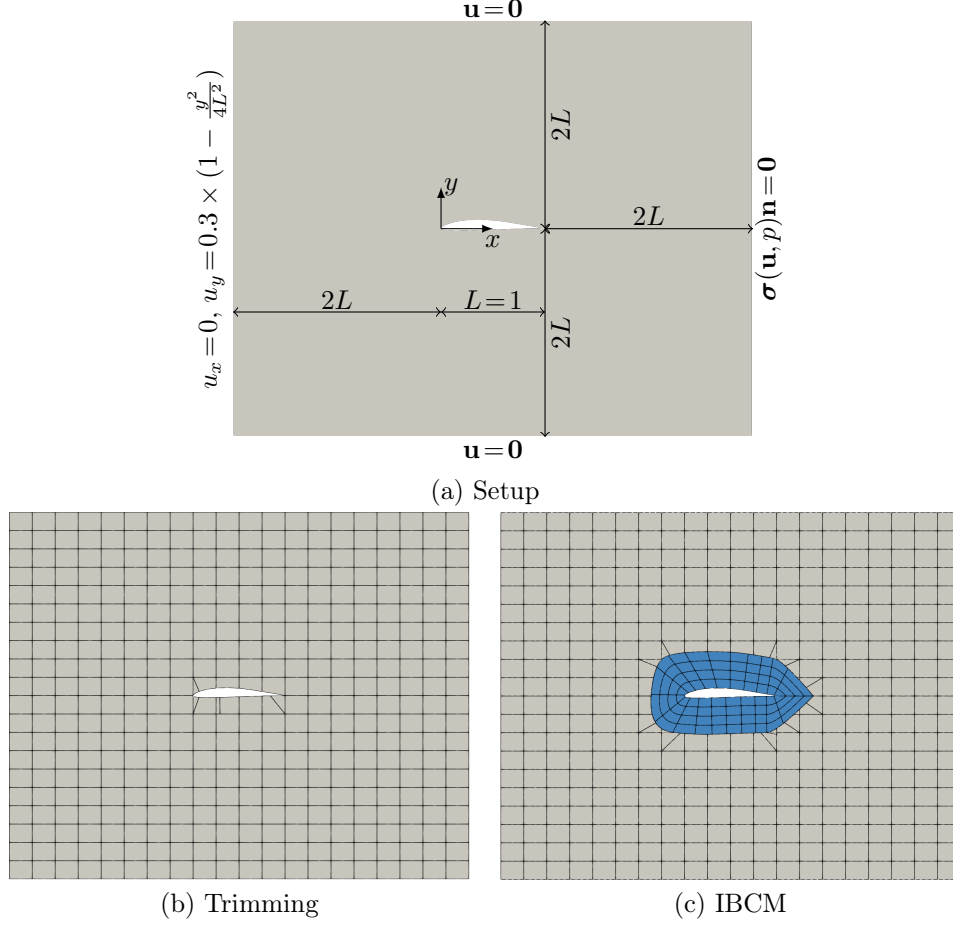


Figure 10: The problem setup (a) and the two geometric constructions (b, c) of the airfoil. Compared to the geometric modeling via pure trimming (a), the immersed boundary-conformal method (IBCM) features an additional conformal mesh around the boundary (b). Note that trimmed elements are reparameterized into multiple integration cells.

different resolutions. We observe that the results using IBCM converge fast (i.e., the results using “mesh 0” and “mesh 3” are very close), whereas the results using trimming vary a lot near the airfoil (i.e., around $x = 0$ and $x = 1$). In summary, with IBCM, we can leverage the geometric flexibility of the overlapping patches to efficiently capture the local features in the solution field without resorting to extensively refining the entire Cartesian grid.

6. Conclusion

In this paper, we present a stabilized isogeometric formulation for the Stokes problem on overlapping multi-patches. The stabilization procedure is a generalization of *minimal stabilization*, which, for the Stokes problem, treats the velocity and pressure separately.

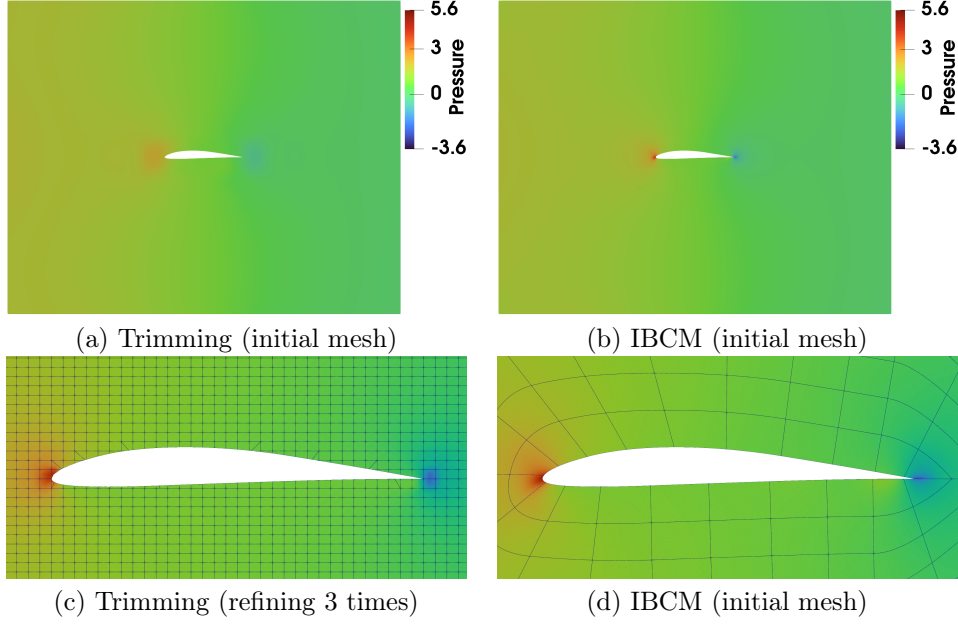


Figure 11: The pressure fields of the Stokes problem around the airfoil. (a, b) The results using the meshes in Figure 10(b, c), respectively, (c) the zoom-in view of the pressure via trimming after refining the initial mesh three times, and (d) the zoom-in view of the pressure via IBCM using the initial mesh.

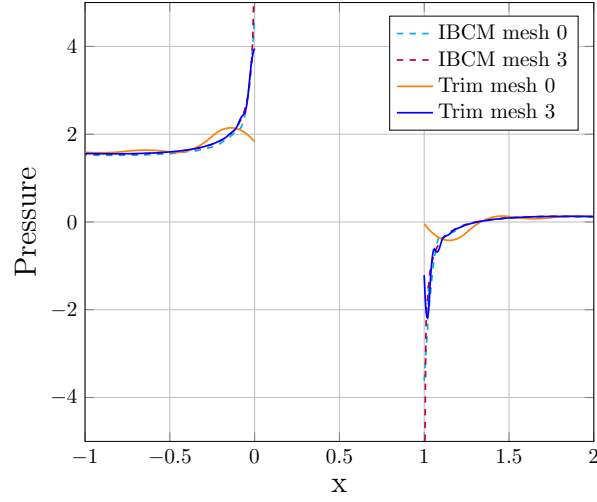


Figure 12: The pressure plot along the line $y = 0$, where the legends “mesh 0” and “mesh 3” mean the initial mesh and the mesh after three dyadic refinements, respectively. Note that the interval $(0, 1)$ corresponds to the airfoil and only part of the entire domain is shown here.

Stabilization of the velocity is only needed on interfaces, where flux terms from bad elements (i.e., cut elements that have small effective measures) are stabilized. On the other

hand, the pressure space is modified on all bad elements and this provides a stable version of the Stokes problem on cut elements without any parameter to be set. Indeed, with one assumption (whose validity can be numerically assessed), we are able to prove the wellposedness and accuracy of our formulation in a completely general setting, allowing for overlaps and mesh cuts of any kind.

In addition to the theoretical study, several numerical examples are presented to show the efficacy, accuracy, and efficiency of the proposed method. The expected convergence is achieved, which agrees with the theory. The accuracy of the pressure jump across interfaces and the conditioning of the linear system are significantly improved by the proposed stabilization procedure, which verifies the necessity of stabilization in practice. The efficiency and geometric flexibility of the proposed method are demonstrated with a special type of overlapping multi-patches that features a layer of conformal mesh around the geometry of interest (called the immersed boundary-conformal method, IBCM). It enables boundary-unfitted methods to naturally and efficiently capture the local solution features around domain boundaries.

In the future, it is promising to investigate minimal stabilization for Kirchhoff-Love shells, especially with the aid of IBCM for rapid geometric modeling and efficient solution procedure. Extension of minimal stabilization to the three-dimensional case via V-rep (the true volume representation as opposed to the dominant B-rep) is another promising and challenging direction. While the theory is mostly dimension-independent, it needs robust and efficient methods and algorithms to make it really happen.

Acknowledgment

X. Wei is supported in part by the National Natural Science Foundation of China (No. 12202269). P. Antolin, and A. Buffa are partially supported by the SNSF of Switzerland through the project “Design- through-Analysis (of PDEs): the litmus test” n. 40B2-0 187094 (BRIDGE Discovery 2019), and the European Union’s Horizon 2020 research and innovation program under Grant Agreement n.862025 (ADAM2).

Appendix A. Technical proofs

Proof of Theorem 21. In order to prove (18), let us show that there exist $c_1, c_2 > 0$ such that, for every $(\mathbf{v}_h, q_h, \boldsymbol{\mu}_h) \in V_h \times \overline{Q}_h \times \Lambda_h$, there exists $(\mathbf{w}_h, r_h, \boldsymbol{\eta}_h) \in V_h \times \overline{Q}_h \times \Lambda_h$ such that $\overline{\mathcal{A}}_h((\mathbf{w}_h, r_h, \boldsymbol{\eta}_h); (\mathbf{v}_h, q_h, \boldsymbol{\mu}_h)) \geq c_1 \|\|(\mathbf{v}_h, q_h, \boldsymbol{\mu}_h)\|\|^2$ and $\|\|(\mathbf{w}_h, r_h, \boldsymbol{\eta}_h)\|\| \leq c_2 \|\|(\mathbf{v}_h, q_h, \boldsymbol{\mu}_h)\|\|$. Let us take $(\mathbf{v}_h, q_h, \boldsymbol{\mu}_h) \in V_h \times \overline{Q}_h \times \Lambda_h$. It holds

$$\begin{aligned} \overline{\mathcal{A}}_h((\mathbf{v}_h, -q_h, -\boldsymbol{\mu}_h); (\mathbf{v}_h, q_h, \boldsymbol{\mu}_h)) &= \sum_{i=0}^N \|D\mathbf{v}_i\|_{L^2(\Omega_i)}^2 \\ &+ \sum_{i=1}^N \sum_{j=0}^{i-1} \gamma^{-1} \left[\left\| \mathbf{h}^{\frac{1}{2}} (-\boldsymbol{\mu}_h + \langle q_h \mathbf{n} \rangle_t) \right\|_{L^2(\Gamma_{ij})}^2 - \left\| \mathbf{h}^{\frac{1}{2}} \langle DR_{ij}^v(\mathbf{v}_h) \mathbf{n} \rangle_t \right\|_{L^2(\Gamma_{ij})}^2 \right]. \end{aligned}$$

Hence, by using Proposition 14 and choosing $\gamma > 0$ large enough,

$$\begin{aligned} \overline{\mathcal{A}}_h((\mathbf{v}_h, -q_h, -\boldsymbol{\mu}_h); (\mathbf{v}_h, q_h, \boldsymbol{\mu}_h)) &\geq (1 - C\gamma^{-1}) \sum_{i=0}^N \|D\mathbf{v}_i\|_{L^2(\Omega_i)}^2 + \gamma^{-1} \sum_{i=1}^N \sum_{j=0}^{i-1} \left\| \mathbf{h}^{\frac{1}{2}} (-\boldsymbol{\mu}_h + \langle q_h \mathbf{n} \rangle_t) \right\|_{L^2(\Gamma_{ij})}^2 \\ &\geq \frac{1}{2} \sum_{i=0}^N \|D\mathbf{v}_i\|_{L^2(\Omega_i)}^2 + \gamma^{-1} \sum_{i=1}^N \sum_{j=0}^{i-1} \left\| \mathbf{h}^{\frac{1}{2}} (-\boldsymbol{\mu}_h + \langle q_h \mathbf{n} \rangle_t) \right\|_{L^2(\Gamma_{ij})}^2. \end{aligned} \quad (\text{A.1})$$

Now, let $\mathbf{w}_h^q \in V_h$ be the supremizer of Lemma 20. Since $b_0(\mathbf{w}_h^q, q_h) \geq C \|q_h\|_{0,h}^2$, we have

$$\begin{aligned} \overline{\mathcal{A}}_h((\mathbf{w}_h^q, 0, 0); (\mathbf{v}_h, q_h, \boldsymbol{\mu}_h)) &\geq \sum_{i=0}^N \int_{\Omega_i} D\mathbf{v}_i : D\mathbf{w}_i^p + C \|q_h\|_{0,h}^2 + \sum_{i=1}^N \sum_{j=0}^{i-1} \int_{\Gamma_{ij}} \boldsymbol{\mu}_h[\mathbf{w}_h^q] \\ &\quad - \sum_{i=1}^N \sum_{j=0}^{i-1} \gamma^{-1} \int_{\Gamma_{ij}} \mathbf{h} \langle DR_{ij}^v(\mathbf{v}_h) \mathbf{n} \rangle_t \langle DR_{ij}^v(\mathbf{w}_h^q) \mathbf{n} \rangle_t \\ &\quad + \sum_{i=1}^N \sum_{j=0}^{i-1} \gamma^{-1} \int_{\Gamma_{ij}} \mathbf{h} (-\boldsymbol{\mu}_h + \langle q_h \mathbf{n} \rangle_t) \langle DR_{ij}^v(\mathbf{w}_h^q) \mathbf{n} \rangle_t. \end{aligned} \quad (\text{A.2})$$

By the Cauchy-Schwarz inequality

$$\begin{aligned} &\sum_{i=1}^N \sum_{j=0}^{i-1} \int_{\Gamma_{ij}} \mathbf{h} \langle DR_{ij}^v(\mathbf{v}_h) \mathbf{n} \rangle_t \langle DR_{ij}^v(\mathbf{w}_h^q) \mathbf{n} \rangle_t \\ &\leq \sum_{i=1}^N \sum_{j=0}^{i-1} \left\| \mathbf{h}^{\frac{1}{2}} \langle DR_{ij}^v(\mathbf{v}_h) \mathbf{n} \rangle_t \right\|_{L^2(\Gamma_{ij})} \left\| \mathbf{h}^{\frac{1}{2}} \langle DR_{ij}^v(\mathbf{w}_h^q) \mathbf{n} \rangle_t \right\|_{L^2(\Gamma_{ij})}, \\ &\sum_{i=1}^N \sum_{j=0}^{i-1} \left| \int_{\Gamma_{ij}} \mathbf{h} (-\boldsymbol{\mu}_h + \langle q_h \mathbf{n} \rangle_t) \langle DR_{ij}^v(\mathbf{w}_h^q) \mathbf{n} \rangle_t \right| \\ &\leq \sum_{i=1}^N \sum_{j=0}^{i-1} \left\| \mathbf{h}^{\frac{1}{2}} (-\boldsymbol{\mu}_h + \langle q_h \mathbf{n} \rangle_t) \right\|_{L^2(\Gamma_{ij})} \left\| \mathbf{h}^{\frac{1}{2}} \langle DR_{ij}^v(\mathbf{w}_h^q) \mathbf{n} \rangle_t \right\|_{L^2(\Gamma_{ij})}. \end{aligned}$$

By using Young's inequality, for $s, \delta > 0$, Proposition 14 and the construction of \mathbf{w}_h^q in the proof of Lemma 20, there exists $C_1 > 0$ such that

$$\begin{aligned} \sum_{i=1}^N \sum_{j=0}^{i-1} \gamma^{-1} \int_{\Gamma_{ij}} \mathbf{h} \langle DR_{ij}^v(\mathbf{v}_h) \mathbf{n} \rangle_t \langle DR_{ij}^v(\mathbf{w}_h^q) \mathbf{n} \rangle_t &\geq -\frac{C_1}{2\gamma s} \sum_{i=0}^N \|D\mathbf{v}_i\|_{L^2(\Omega_i)}^2 - \frac{sC_1}{2\gamma} \|q_h\|_{0,h}^2, \\ \sum_{i=1}^N \sum_{j=0}^{i-1} \gamma^{-1} \int_{\Gamma_{ij}} \mathbf{h} (-\boldsymbol{\mu}_h + \langle q_h \mathbf{n} \rangle_t) \langle DR_{ij}^v(\mathbf{w}_h^q) \mathbf{n} \rangle_t &\geq -\frac{C_1}{2\gamma \delta} \sum_{i=1}^N \sum_{j=0}^{i-1} \left\| \mathbf{h}^{\frac{1}{2}} (-\boldsymbol{\mu}_h + \langle q_h \mathbf{n} \rangle_t) \right\|_{L^2(\Gamma_{ij})}^2 \\ &\quad - \frac{\delta C_1}{2\gamma} \|q_h\|_{0,h}^2. \end{aligned}$$

From the Cauchy-Schwarz inequality, the construction of \mathbf{w}_h^q , and Young's inequality, there exists $C_2 > 0$ such that, for $\varepsilon > 0$,

$$\sum_{i=0}^N \int_{\Omega_i} D\mathbf{v}_i : D\mathbf{w}_i^p \geq -\frac{C_2}{2\varepsilon} \sum_{i=0}^N \|D\mathbf{v}_i\|_{L^2(\Omega_i)}^2 - \frac{\varepsilon C_2}{2} \|q_h\|_{0,h}^2.$$

In an analogous fashion, there exists $C_3 > 0$ such that, for $r > 0$,

$$\sum_{i=1}^N \sum_{j=0}^{i-1} \int_{\Gamma_{ij}} \boldsymbol{\mu}_h[\mathbf{w}_h^q] \geq -\frac{C_3}{2r} \sum_{i=1}^N \sum_{j=0}^{i-1} \left\| \mathbf{h}^{\frac{1}{2}} \boldsymbol{\mu}_h \right\|_{L^2(\Gamma_{ij})}^2 - \frac{rC_3}{2} \|q_h\|_{0,h}^2.$$

Let us go back to (A.2). We have

$$\begin{aligned} \overline{\mathcal{A}}_h((\mathbf{w}_h^q, 0, \mathbf{0}); (\mathbf{v}_h, q_h, \boldsymbol{\mu}_h)) &\geq -\frac{C_2}{2\varepsilon} \sum_{i=0}^N \|D\mathbf{v}_i\|_{L^2(\Omega_i)}^2 - \frac{\varepsilon C_2}{2} \|q_h\|_{0,h}^2 + C \|q_h\|_{0,h}^2 \\ &\quad - \frac{C_3}{2r} \sum_{i=1}^N \sum_{j=0}^{i-1} \left\| \mathbf{h}^{\frac{1}{2}} \boldsymbol{\mu}_h \right\|_{L^2(\Gamma_{ij})}^2 - \frac{rC_3}{2} \|q_h\|_{0,h}^2 - \frac{C_1}{2\gamma s} \sum_{i=0}^N \|D\mathbf{v}_i\|_{L^2(\Omega_i)}^2 \\ &\quad - \frac{sC_1}{2\gamma} \|q_h\|_{0,h}^2 - \frac{C_1}{2\gamma\delta} \sum_{i=1}^N \sum_{j=0}^{i-1} \left\| \mathbf{h}^{\frac{1}{2}} (-\boldsymbol{\mu}_h + \langle q_h \mathbf{n} \rangle_t) \right\|_{L^2(\Gamma_{ij})}^2 - \frac{\delta C_1}{2\gamma} \|q_h\|_{0,h}^2 \\ &= \left(C - \frac{\varepsilon C_2}{2} - \frac{rC_3}{2} - \frac{sC_1}{2\gamma} - \frac{\delta C_1}{2\gamma} \right) \|q_h\|_{0,h}^2 + \left(-\frac{C_2}{2\varepsilon} - \frac{C_1}{2\gamma s} \right) \sum_{i=0}^N \|D\mathbf{v}_i\|_{L^2(\Omega_i)}^2 \\ &\quad - \frac{C_1}{2\gamma\delta} \sum_{i=1}^N \sum_{j=0}^{i-1} \left\| \mathbf{h}^{\frac{1}{2}} (-\boldsymbol{\mu}_h + \langle q_h \mathbf{n} \rangle_t) \right\|_{L^2(\Gamma_{ij})}^2 - \frac{C_3}{2r} \sum_{i=1}^N \sum_{j=0}^{i-1} \left\| \mathbf{h}^{\frac{1}{2}} \boldsymbol{\mu}_h \right\|_{L^2(\Gamma_{ij})}^2. \end{aligned}$$

Let $\varepsilon, r, s, \delta > 0$ be small enough such that $C - \frac{\varepsilon C_2}{2} - \frac{rC_3}{2} - \frac{sC_1}{2\gamma} - \frac{\delta C_1}{2\gamma} \geq \frac{C}{2}$. Hence, there exist $C_4, C_5, C_6 > 0$ such that

$$\begin{aligned} \overline{\mathcal{A}}_h((\mathbf{w}_h^q, 0, \mathbf{0}); (\mathbf{v}_h, q_h, \boldsymbol{\mu}_h)) &\geq \frac{C}{2} \|q_h\|_{0,h}^2 - C_4 \sum_{i=0}^N \|D\mathbf{v}_i\|_{L^2(\Omega_i)}^2 \\ &\quad - C_5 \sum_{i=1}^N \sum_{j=0}^{i-1} \left\| \mathbf{h}^{\frac{1}{2}} (-\boldsymbol{\mu}_h + \langle q_h \mathbf{n} \rangle_t) \right\|_{L^2(\Gamma_{ij})}^2 - C_6 \sum_{i=1}^N \sum_{j=0}^{i-1} \left\| \mathbf{h}^{\frac{1}{2}} \boldsymbol{\mu}_h \right\|_{L^2(\Gamma_{ij})}^2. \end{aligned} \tag{A.3}$$

Let $P_h : \bigoplus_{0 \leq j < i \leq N} L^2(\Gamma_{ij}) \rightarrow \Lambda_h$ be the L^2 -orthogonal projection. From condition (10), we have $\mathbf{h}^{-1}[\mathbf{v}_h]_{\Gamma_{ij}} = P_h \mathbf{h}^{-1}[\mathbf{v}_h]_{\Gamma_{ij}}$, for every $0 \leq j < i \leq N$. Therefore, from the

Cauchy-Schwartz inequality, we have

$$\begin{aligned} \overline{\mathcal{A}}_h((\mathbf{0}, 0, P_h \mathbf{h}^{-1}[\mathbf{v}_h]); (\mathbf{v}_h, q_h, \boldsymbol{\mu}_h)) &\geq \sum_{i=1}^N \sum_{j=0}^{i-1} \left\| \mathbf{h}^{-\frac{1}{2}}[\mathbf{v}_h] \right\|_{L^2(\Gamma_{ij})}^2 \\ &\quad - \gamma^{-1} \left(\sum_{i=1}^N \sum_{j=0}^{i-1} \left\| \mathbf{h}^{\frac{1}{2}} \langle DR_{ij}^v(\mathbf{v}_h) \mathbf{n} \rangle_t \right\|_{L^2(\Gamma_{ij})} \left\| \mathbf{h}^{-\frac{1}{2}}[\mathbf{v}_h] \right\|_{L^2(\Gamma_{ij})} \right. \\ &\quad \left. + \sum_{i=1}^N \sum_{j=0}^{i-1} \left\| \mathbf{h}^{\frac{1}{2}}(-\boldsymbol{\mu}_h + \langle q_h \mathbf{n} \rangle_t) \right\|_{L^2(\Gamma_{ij})} \left\| \mathbf{h}^{-\frac{1}{2}}[\mathbf{v}_h] \right\|_{L^2(\Gamma_{ij})} \right). \end{aligned}$$

By Proposition 14 and Young's inequality, there exists $C_7 > 0$ such that, for $a, b > 0$,

$$\begin{aligned} - \sum_{i=1}^N \sum_{j=0}^{i-1} \left\| \mathbf{h}^{\frac{1}{2}} \langle DR_h^v(\mathbf{v}_h) \mathbf{n} \rangle_t \right\|_{L^2(\Gamma_{ij})} \left\| \mathbf{h}^{-\frac{1}{2}}[\mathbf{v}_h] \right\|_{L^2(\Gamma_{ij})} &\geq - \frac{C_7}{2a} \sum_{i=0}^N \|D\mathbf{v}_i\|_{L^2(\Omega_i)}^2 \\ &\quad - \frac{aC_7}{2} \sum_{i=1}^N \sum_{j=0}^{i-1} \left\| \mathbf{h}^{-\frac{1}{2}}[\mathbf{v}_h] \right\|_{L^2(\Gamma_{ij})}^2, \\ - \sum_{i=1}^N \sum_{j=0}^{i-1} \left\| \mathbf{h}^{\frac{1}{2}}(-\boldsymbol{\mu}_h + \langle q_h \mathbf{n} \rangle_t) \right\|_{L^2(\Gamma_{ij})} \left\| \mathbf{h}^{-\frac{1}{2}}[\mathbf{v}_h] \right\|_{L^2(\Gamma_{ij})} &\geq - \frac{1}{2b} \sum_{i=1}^N \sum_{j=0}^{i-1} \left\| \mathbf{h}^{\frac{1}{2}}(-\boldsymbol{\mu}_h + \langle q_h \mathbf{n} \rangle_t) \right\|_{L^2(\Gamma_{ij})}^2 \\ &\quad - \frac{b}{2} \sum_{i=1}^N \sum_{j=0}^{i-1} \left\| \mathbf{h}^{-\frac{1}{2}}[\mathbf{v}_h] \right\|_{L^2(\Gamma_{ij})}^2. \end{aligned}$$

Thus,

$$\begin{aligned} \overline{\mathcal{A}}_h((\mathbf{0}, 0, P_h \mathbf{h}^{-1}[\mathbf{v}_h]); (\mathbf{v}_h, q_h, \boldsymbol{\mu}_h)) &\geq \left(1 - \frac{aC_7}{2\gamma} - \frac{b}{2\gamma}\right) \sum_{i=1}^N \sum_{j=0}^{i-1} \left\| \mathbf{h}^{-\frac{1}{2}}[\mathbf{v}_h] \right\|_{L^2(\Gamma_{ij})}^2 \\ &\quad - \frac{C_7}{2a\gamma} \sum_{i=0}^N \|D\mathbf{v}_i\|_{L^2(\Omega_i)}^2 - \frac{1}{2b\gamma} \sum_{i=1}^N \sum_{j=0}^{i-1} \left\| \mathbf{h}^{\frac{1}{2}}(-\boldsymbol{\mu}_h + \langle q_h \mathbf{n} \rangle_t) \right\|_{L^2(\Gamma_{ij})}^2. \end{aligned}$$

Let us choose $a, b > 0$ small enough such that $1 - \frac{aC_7}{2\gamma} - \frac{b}{2\gamma} \geq \frac{1}{2}$. Hence, there exist $C_8, C_9 > 0$ such that

$$\begin{aligned} \overline{\mathcal{A}}_h((\mathbf{0}, 0, P_h \mathbf{h}^{-1}[\mathbf{v}_h]); (\mathbf{v}_h, q_h, \boldsymbol{\mu}_h)) &\geq \frac{1}{2} \sum_{i=1}^N \sum_{j=0}^{i-1} \left\| \mathbf{h}^{-\frac{1}{2}}[\mathbf{v}_h] \right\|_{L^2(\Gamma_{ij})}^2 - C_8 \sum_{i=0}^N \|D\mathbf{v}_i\|_{L^2(\Omega_i)}^2 \\ &\quad - C_9 \sum_{i=1}^N \sum_{j=0}^{i-1} \left\| \mathbf{h}^{\frac{1}{2}}(-\boldsymbol{\mu}_h + \langle q_h \mathbf{n} \rangle_t) \right\|_{L^2(\Gamma_{ij})}^2. \end{aligned} \tag{A.4}$$

Let us put together (A.1), (A.3), (A.4). For $k, \eta > 0$, we have

$$\begin{aligned} \overline{\mathcal{A}}_h((\mathbf{v}_h + k\mathbf{w}_h^q, -q_h, -\boldsymbol{\mu}_h + \eta P_h \mathbf{h}^{-1}[\mathbf{v}_h]); (\mathbf{v}_h, q_h, \boldsymbol{\mu}_h)) &\geq \left(\frac{1}{2} - kC_4 - \eta C_8\right) \sum_{i=0}^N \|D\mathbf{v}_i\|_{L^2(\Omega_i)}^2 \\ &+ \left(\frac{1}{\gamma} - kC_5 - \eta C_9\right) \sum_{i=1}^N \sum_{j=0}^{i-1} \left\| \mathbf{h}^{\frac{1}{2}} (-\boldsymbol{\mu}_h + \langle q_h \mathbf{n} \rangle_t) \right\|_{L^2(\Gamma_{ij})}^2 + \frac{kC}{2} \|q_h\|_{0,h}^2 \\ &- kC_6 \sum_{i=1}^N \sum_{j=0}^{i-1} \left\| \mathbf{h}^{\frac{1}{2}} \boldsymbol{\mu}_h \right\|_{L^2(\Gamma_{ij})}^2 + \frac{\eta}{2} \sum_{i=1}^N \sum_{j=0}^{i-1} \left\| \mathbf{h}^{-\frac{1}{2}} [\mathbf{v}_h] \right\|_{L^2(\Gamma_{ij})}^2. \end{aligned}$$

From Proposition 12, there exists $C_{10} > 0$ such that

$$\begin{aligned} \overline{\mathcal{A}}_h((\mathbf{v}_h + k\mathbf{w}_h^q, -q_h, -\boldsymbol{\mu}_h + \eta P_h \mathbf{h}^{-1}[\mathbf{v}_h]); (\mathbf{v}_h, q_h, \boldsymbol{\mu}_h)) &\geq \left(\frac{1}{2} - kC_4 - \eta C_8\right) \sum_{i=0}^N \|D\mathbf{v}_i\|_{L^2(\Omega_i)}^2 \\ &+ \left(\frac{1}{\gamma} - kC_5 - \eta C_9\right) \sum_{i=1}^N \sum_{j=0}^{i-1} \left\| \mathbf{h}^{\frac{1}{2}} (-\boldsymbol{\mu}_h + \langle q_h \mathbf{n} \rangle_t) \right\|_{L^2(\Gamma_{ij})}^2 + \frac{k}{4C_{10}} \sum_{i=1}^N \sum_{j=0}^{i-1} \left\| \mathbf{h}^{\frac{1}{2}} \langle q_h \rangle_t \right\|_{L^2(\Gamma_{ij})}^2 \\ &+ \frac{kC}{4} \|q_h\|_{0,h}^2 - kC_6 \sum_{i=1}^N \sum_{j=0}^{i-1} \left\| \mathbf{h}^{\frac{1}{2}} \boldsymbol{\mu}_h \right\|_{L^2(\Gamma_{ij})}^2 + \frac{\eta}{2} \sum_{i=1}^N \sum_{j=0}^{i-1} \left\| \mathbf{h}^{-\frac{1}{2}} [\mathbf{v}_h] \right\|_{L^2(\Gamma_{ij})}^2. \end{aligned} \tag{A.5}$$

Let $C_{11} := \frac{4}{kC_{10}}$ and $C_{12} := \frac{1}{\gamma} - kC_5 - \eta C_9$, and observe that, by Young inequality, for any $\ell > 0$,

$$\left\| \mathbf{h}^{\frac{1}{2}} (-\boldsymbol{\mu}_h + \langle q_h \mathbf{n} \rangle_t) \right\|_{L^2(\Gamma_{ij})}^2 \geq (1 - \ell) \left\| \mathbf{h}^{\frac{1}{2}} \langle q_h \rangle_t \right\|_{L^2(\Gamma_{ij})}^2 + \left(1 - \frac{1}{\ell}\right) \left\| \mathbf{h}^{\frac{1}{2}} \boldsymbol{\mu}_h \right\|_{L^2(\Gamma_{ij})}^2.$$

By using $\left\| \mathbf{h}^{\frac{1}{2}} \langle q_h \rangle_t \right\|_{L^2(\Gamma_{ij})}^2 = \left\| \mathbf{h}^{\frac{1}{2}} \langle q_h \rangle_t \right\|_{L^2(\Gamma_{ij})}^2$, we have

$$\begin{aligned} &C_{11} \sum_{i=1}^N \sum_{j=0}^{i-1} \left\| \mathbf{h}^{\frac{1}{2}} \langle q_h \rangle_t \right\|_{L^2(\Gamma_{ij})}^2 + C_{12} \sum_{i=1}^N \sum_{j=0}^{i-1} \left\| \mathbf{h}^{\frac{1}{2}} (-\boldsymbol{\mu}_h + \langle q_h \mathbf{n} \rangle_t) \right\|_{L^2(\Gamma_{ij})}^2 \\ &\geq C_{12} \sum_{i=1}^N \sum_{j=0}^{i-1} \left(\left(\frac{C_{11}}{C_{12}} + 1 - \ell \right) \left\| \mathbf{h}^{\frac{1}{2}} \langle q_h \rangle_t \right\|_{L^2(\Gamma_{ij})}^2 + \left(1 - \frac{1}{\ell}\right) \left\| \mathbf{h}^{\frac{1}{2}} \boldsymbol{\mu}_h \right\|_{L^2(\Gamma_{ij})}^2 \right). \end{aligned} \tag{A.6}$$

By plugging (A.6) back into (A.5), we have

$$\begin{aligned} \overline{\mathcal{A}}_h((\mathbf{v}_h + k\mathbf{w}_h^q, -q_h, -\boldsymbol{\mu}_h + \eta P_h \mathbf{h}^{-1}[\mathbf{v}_h]); (\mathbf{v}_h, q_h, \boldsymbol{\mu}_h)) &\geq \left(\frac{1}{2} - kC_4 - \eta C_8\right) \sum_{i=0}^N \|D\mathbf{v}_i\|_{L^2(\Omega_i)}^2 \\ &+ C_{12} \left(\frac{C_{11}}{C_{12}} + 1 - \ell \right) \sum_{i=1}^N \sum_{j=0}^{i-1} \left\| \mathbf{h}^{\frac{1}{2}} \langle q_h \rangle_t \right\|_{L^2(\Gamma_{ij})}^2 + \left(C_{12} \left(1 - \frac{1}{\ell}\right) - kC_6 \right) \sum_{i=1}^N \sum_{j=0}^{i-1} \left\| \mathbf{h}^{\frac{1}{2}} \boldsymbol{\mu}_h \right\|_{L^2(\Gamma_{ij})}^2 \\ &+ \frac{kC}{4} \|q_h\|_{0,h}^2 + \frac{\eta}{2} \sum_{i=1}^N \sum_{j=0}^{i-1} \left\| \mathbf{h}^{-\frac{1}{2}} [\mathbf{v}_h] \right\|_{L^2(\Gamma_{ij})}^2. \end{aligned}$$

We require $1 < \ell < \frac{C_{11}}{C_{12}} + 1$ and k, η to be small enough so that $\frac{1}{2} - kC_4 - \eta C_8 \geq \frac{1}{4}$, $C_{12} \left(\frac{C_{11}}{C_{12}} + 1 - \ell \right) \geq C_{13}$, $C_{12} \left(1 - \frac{1}{\ell} \right) - kC_6 \geq C_{14}$, for some $C_{13}, C_{14} > 0$. Note that the choice of ℓ depends on k and η . On the other hand, there exist $C_{15}, C_{16} > 0$ such that $\frac{kC}{4} \geq C_{15}$ and $\frac{\eta}{2} \geq C_{16}$. Hence,

$$\begin{aligned} \overline{\mathcal{A}}_h \left((\mathbf{v}_h + k\mathbf{w}_h^q, -q_h, -\boldsymbol{\mu}_h + \eta P_h \mathbf{h}^{-1}[\mathbf{v}_h]) ; (\mathbf{v}_h, q_h, \boldsymbol{\mu}_h) \right) &\geq \frac{1}{4} \sum_{i=0}^N \|D\mathbf{v}_i\|_{L^2(\Omega_i)}^2 \\ &+ C_{13} \sum_{i=1}^N \sum_{j=0}^{i-1} \left\| \mathbf{h}^{\frac{1}{2}} \langle q_h \rangle_t \right\|_{L^2(\Gamma_{ij})}^2 + C_{14} \sum_{i=1}^N \sum_{j=0}^{i-1} \left\| \mathbf{h}^{\frac{1}{2}} \boldsymbol{\mu}_h \right\|_{L^2(\Gamma_{ij})}^2 \\ &+ C_{15} \|q_h\|_{0,h}^2 + C_{16} \sum_{i=1}^N \sum_{j=0}^{i-1} \left\| \mathbf{h}^{-\frac{1}{2}}[\mathbf{v}_h] \right\|_{L^2(\Gamma_{ij})}^2. \end{aligned}$$

Finally, the stability property of \mathbf{w}_h^q , namely $\|\mathbf{w}_h^q\|_{1,h} \leq C \|q_h\|_{0,h}$, entails

$$\left\| (\mathbf{v}_h + k\mathbf{w}_h^q, -q_h, -\boldsymbol{\mu}_h + \eta P_h \mathbf{h}^{-1}[\mathbf{v}_h]) \right\| \leq C \left\| (\mathbf{v}_h, q_h, \boldsymbol{\mu}_h) \right\|.$$

□

References

- [1] A. Buffa, R. Puppi, R. Vázquez, A minimal stabilization procedure for isogeometric methods on trimmed geometries, *SIAM Journal on Numerical Analysis* 58 (5) (2020) 2711–2735.
- [2] T. J. R. Hughes, J. A. Cottrell, Y. Bazilevs, Isogeometric analysis: CAD, finite elements, NURBS, exact geometry and mesh refinement, *Computer Methods in Applied Mechanics and Engineering* 194 (39) (2005) 4135–4195.
- [3] M.-C. Hsu, C. Wang, A. J. Herrema, D. Schillinger, A. Ghoshal, Y. Bazilevs, An interactive geometry modeling and parametric design platform for isogeometric analysis, *Computers & Mathematics with Applications* 70 (7) (2015) 1481–1500.
- [4] Y. Lai, Y. J. Zhang, L. Liu, X. Wei, E. F., J. Lua, Integrating CAD with Abaqus: A practical isogeometric analysis software platform for industrial applications, *Computers & Mathematics with Applications* 74 (7) (2017) 1648–1660.
- [5] H. Casquero, X. Wei, D. Toshniwal, A. Li, T. J. R. Hughes, J. Kiendl, Y. J. Zhang, Seamless integration of design and Kirchhoff–Love shell analysis using analysis-suitable unstructured T-splines, *Computer Methods in Applied Mechanics and Engineering* 360 (2020) 112765.
- [6] D. Kamensky, M.-C. Hsu, D. Schillinger, J. A. Evans, A. Aggarwal, Y. Bazilevs, M. S. Sacks, T. J. R. Hughes, An immersogeometric variational framework for fluid–structure interaction: Application to bioprosthetic heart valves, *Computer Methods in Applied Mechanics and Engineering* 284 (2015) 1005–1053.
- [7] A. Li, X. Chai, G. Yang, Y. J. Zhang, An isogeometric analysis computational platform for material transport simulations in complex neurite networks, *Molecular & cellular biomechanics* 16 (2) (2019) 123–140.
- [8] J. A. Evans, Y. Bazilevs, I. Babuška, T. J. R. Hughes, n-Widths, sup–infs, and optimality ratios for the k-version of the isogeometric finite element method, *Computer Methods in Applied Mechanics and Engineering* 198 (21) (2009) 1726–1741.
- [9] S. Lipton, J. A. Evans, Y. Bazilevs, T. Elguedj, T. J. R. Hughes, Robustness of isogeometric structural discretizations under severe mesh distortion, *Computer Methods in Applied Mechanics and Engineering* 199 (5) (2010) 357–373.
- [10] T. Martin, E. Cohen, R. M. Kirby, Volumetric parameterization and trivariate B-spline fitting using harmonic functions, *Computer Aided Geometric Design* 26 (6) (2009) 648–664.
- [11] Y. Zhang, W. Wang, T. J. R. Hughes, Solid T-spline construction from boundary representations for genus-zero geometry, *Computer Methods in Applied Mechanics and Engineering* 249–252 (2012) 185–197.
- [12] Y. Zhang, W. Wang, T. J. R. Hughes, Conformal solid T-spline construction from boundary T-spline representations, *Computational Mechanics* 51 (6) (2013) 1051–1059.
- [13] F. Massarwi, G. Elber, A B-spline based framework for volumetric object modeling, *Computer Aided Design* 78 (2016) 36–47.
- [14] P. Antolín, A. Buffa, M. Martinelli, Isogeometric analysis on V-reps: first results, *Computer Methods in Applied Mechanics and Engineering* 355 (2019) 976–1002.
- [15] J. Parvizian, A. Düster, E. Rank, Finite cell method: h- and p- extension for embedded domain methods in solid mechanics, *Computational Mechanics* 41 (2007) 122–133.
- [16] E. Burman, S. Claus, P. Hansbo, M. G. Larson, A. Massing, CutFEM: Discretizing geometry and partial differential equations, *International Journal for Numerical Methods in Engineering* 104 (7) (2015) 472–501.
- [17] A. Main, G. Scovazzi, The shifted boundary method for embedded domain computations. Part I: Poisson and Stokes problems, *Journal of Computational Physics* 372 (2018) 972–995.
- [18] S. Badia, F. Verdugo, A. F. Martín, The aggregated unfitted finite element method for elliptic problems, *Computer Methods in Applied Mechanics and Engineering* 336 (2018) 533–553.
- [19] S. Badia, E. Neiva, F. Verdugo, Robust high-order unfitted finite elements by interpolation-based discrete extension, *Computers & Mathematics with Applications* 127 (2022) 105–126.
- [20] F. de Prenter, C. V. Verhoosel, E. H. van Brummelen, M. G. Larson, S. Badia, Stability and conditioning of immersed finite element methods: Analysis and remedies, *Archives of Computational Methods in Engineering* (2023) 1–40.
- [21] L. Kudela, N. Zander, S. Kollmannsberger, E. Rank, Smart octrees: Accurately integrating discontinuous functions in 3D, *Computer Methods in Applied Mechanics and Engineering* 306 (2016) 406–426.
- [22] S. C. Divi, C. V. Verhoosel, F. Auricchio, A. Reali, E. H. van Brummelen, Error-estimate-based

- adaptive integration for immersed isogeometric analysis, *Computers & Mathematics with Applications* 80 (11) (2020) 2481–2516.
- [23] D. Gunderman, K. Weiss, J. A. Evans, High-accuracy mesh-free quadrature for trimmed parametric surfaces and volumes, *Computer-Aided Design* 141 (2021) 103093.
 - [24] W. Garhum, A. Düster, Non-negative moment fitting quadrature for cut finite elements and cells undergoing large deformations, *Computational Mechanics* 70 (5) (2022) 1059–1081.
 - [25] R. I. Saye, High-order quadrature on multi-component domains implicitly defined by multivariate polynomials, *Journal of Computational Physics* 448 (2022) 110720.
 - [26] P. Antolin, X. Wei, A. Buffa, Robust numerical integration on curved polyhedra based on folded decompositions, *Computer Methods in Applied Mechanics and Engineering* 395 (2022) 114948.
 - [27] P. Antolin, T. Hirschler, Quadrature-free immersed isogeometric analysis, *Engineering with Computers* 38 (5) (2022) 4475–4499.
 - [28] M. Ruess, D. Schillinger, Y. Bazilevs, V. Varduhn, E. Rank, Weakly enforced essential boundary conditions for NURBS-embedded and trimmed NURBS geometries on the basis of the finite cell method, *International Journal for Numerical Methods in Engineering* 95 (10) (2013) 811–846.
 - [29] X. Wei, B. Marussig, P. Antolin, A. Buffa, Immersed boundary-conformal isogeometric method for linear elliptic problems, *Computational Mechanics* 68 (2009) 1385–1405.
 - [30] B. Marussig, T. J. Hughes, A review of trimming in isogeometric analysis: Challenges, data exchange and simulation aspects, *Archives of computational methods in engineering* 25 (2018) 1059–1127.
 - [31] T. Teschemacher, A. M. Bauer, T. Oberbichler, M. Breitenberger, R. Rossi, R. Wüchner, K.-U. Bletzinger, Realization of CAD-integrated shell simulation based on isogeometric B-Rep analysis, *Advanced Modeling and Simulation in Engineering Sciences* 5 (1) (2018) 19.
 - [32] L. F. Leidinger, M. Breitenberger, A. M. Bauer, S. Hartmann, R. Wüchner, K.-U. Bletzinger, F. Duddeck, L. Song, Explicit dynamic isogeometric B-Rep analysis of penalty-coupled trimmed NURBS shells, *Computer Methods in Applied Mechanics and Engineering* 351 (2019) 891–927.
 - [33] D. Schillinger, L. Dedè, M. A. Scott, J. A. Evans, M. J. Borden, E. Rank, T. R. Hughes, An isogeometric design-through-analysis methodology based on adaptive hierarchical refinement of NURBS, immersed boundary methods, and T-spline CAD surfaces, *Computer Methods in Applied Mechanics and Engineering* 249–252 (2012) 116–150.
 - [34] P. Antolin, A. Buffa, R. Puppi, X. Wei, Overlapping multipatch isogeometric method with minimal stabilization, *SIAM Journal on Scientific Computing* 43 (1) (2021) A330–A354.
 - [35] R. Puppi, Isogeometric discretizations of the Stokes problem on trimmed geometries, *arXiv:2012.15582* (2022).
 - [36] J. Guzmán, M. Olshanskii, Inf-sup stability of geometrically unfitted Stokes finite elements, *Mathematics of Computation* 87 (313) (2018) 2091–2112.
 - [37] S. Badia, A. F. Martin, F. Verdugo, Mixed aggregated finite element methods for the unfitted discretization of the Stokes problem, *SIAM journal on scientific computing* 40 (6) (2018) B1541–B1576.
 - [38] E. Burman, G. Delay, A. Ern, An unfitted hybrid high-order method for the Stokes interface problem, *IMA Journal of Numerical Analysis* 41 (4) (2021) 2362–2387.
 - [39] A. Johansson, B. Kehlet, M. G. Larson, A. Logg, Multimesh finite element methods: Solving PDEs on multiple intersecting meshes, *Computer Methods in Applied Mechanics and Engineering* 343 (2019) 672–689.
 - [40] A. Johansson, M. G. Larson, A. Logg, *A Multimesh Finite Element Method for the Stokes Problem*, Springer International Publishing, 2020, pp. 189–198.
 - [41] P. Antolin, A. Buffa, E. Cirillo, Region extraction in mesh intersection, *Computer-Aided Design* 156 (2023) 103448.
 - [42] R. A. Adams, J. J. F. Fournier, *Sobolev spaces*, 2nd Edition, Vol. 140 of *Pure and Applied Mathematics* (Amsterdam), Elsevier/Academic Press, Amsterdam, 2003.
 - [43] L. Tartar, An introduction to Sobolev spaces and interpolation spaces, Vol. 3 of *Lecture Notes of the Unione Matematica Italiana*, Springer, Berlin; UMI, Bologna, 2007.
 - [44] T. Lyche, K. Mørken, *Spline methods draft* (2008).
 - [45] Y. Bazilevs, L. Beirão da Veiga, J. A. Cottrell, T. J. R. Hughes, G. Sangalli, Isogeometric analysis: Approximation, stability and error estimates for h -refined meshes, *Mathematical Models and Methods in Applied Sciences* 16 (7) (2006) 1031–1090.
 - [46] J. A. Cottrell, T. J. R. Hughes, Y. Bazilevs, *Isogeometric analysis: Toward integration of CAD and FEA*, John Wiley & Sons, Ltd., 2009.
 - [47] A. Johansson, M. G. Larson, A. Logg, Multimesh finite elements with flexible mesh sizes, *Computer Methods in Applied Mechanics and Engineering* 372 (2020) 113420.

- [48] M. Fournié, A. Lozinski, Stability and optimal convergence of unfitted extended finite element methods with Lagrange multipliers for the Stokes equations, in: Geometrically unfitted finite element methods and applications, Vol. 121 of Lecture Notes in Computational Science and Engineering, Springer, 2017, pp. 143–182.
- [49] L. Beirão da Veiga, A. Buffa, G. Sangalli, R. Vázquez, Mathematical analysis of variational isogeometric methods, *Acta Numerica* 23 (2014) 157–287.
- [50] A. Buffa, C. de Falco, G. Sangalli, IsoGeometric Analysis: Stable elements for the 2D Stokes equation, *Internat. J. Numer. Methods Fluids* 65 (11-12) (2011) 1407–1422.
- [51] A. Quarteroni, A. Valli, Domain decomposition methods for partial differential equations, Numerical Mathematics and Scientific Computation, Oxford University Press, 1999.
- [52] J. A. Evans, T. J. R. Hughes, Isogeometric divergence-conforming B-splines for the steady Navier-Stokes equations, *Mathematical Models and Methods in Applied Sciences* 23 (8) (2013) 1421–1478.
- [53] A. Buffa, E. M. Garau, C. Giannelli, G. Sangalli, On quasi-interpolation operators in spline spaces, in: Building bridges: connections and challenges in modern approaches to numerical partial differential equations, Vol. 114 of Lecture Notes in Computational Science and Engineering, Springer, 2016, pp. 73–91.
- [54] R. Stenberg, On some techniques for approximating boundary conditions in the finite element method, *Journal of Computational and Applied Mathematics* 63 (1) (1995) 139–148.
- [55] F. J. Sayas, T. S. Brown, M. E. Hassell, Variational techniques for elliptic partial differential equations, CRC Press, 2019.
- [56] A. Ern, J.-L. Guermond, Theory and practice of finite elements, Vol. 159 of Applied Mathematical Sciences, Springer-Verlag, 2004.
- [57] D. Boffi, F. Brezzi, M. Fortin, Mixed finite element methods and applications, Vol. 44 of Springer Series in Computational Mathematics, Springer, Heidelberg, 2013.